

**CHARACTERIZATION OF FILTER CAKE BUILDUP AND CLEANUP UNDER  
DYNAMIC FLUID LOSS CONDITIONS**

A Thesis

by

TAKWE YANGO

Submitted to the Office of Graduate Studies of  
Texas A&M University  
in partial fulfillment of the requirements for the degree of

MASTER OF SCIENCE

August 2011

Major Subject: Petroleum Engineering

Characterization of Filter Cake Buildup and Cleanup under Dynamic Fluid Loss

Conditions

Copyright 2011 Takwe Yango

**CHARACTERIZATION OF FILTER CAKE BUILDUP AND CLEANUP UNDER  
DYNAMIC FLUID LOSS CONDITIONS**

A Thesis

by

TAKWE YANGO

Submitted to the Office of Graduate Studies of  
Texas A&M University  
in partial fulfillment of the requirements for the degree of

**MASTER OF SCIENCE**

Approved by:

Co-Chairs of Committee, Ding Zhu

A. Dan Hill

Committee Members, Maria Barrufet

Head of Department, Stephen Holditch

August 2011

Major Subject: Petroleum Engineering

**ABSTRACT**

Characterization of Filter Cake Buildup and Cleanup under Dynamic Fluid Loss  
Conditions.

(August 2011)

Takwe Yango, B.S., Oklahoma State University

Co-Chairs of Advisory Committee: Dr. Ding Zhu  
Dr. A. Dan Hill

Hydraulic fracturing is a popular stimulation method in tight gas and shale gas reservoirs that uses a viscous fluid to fracture the reservoir rock and uniformly transport proppant to create a highly conductive path that is kept open by the proppant after fracturing. This method is used to improve the productivity of the otherwise low permeability reservoirs. Hydraulic fracturing, though in general beneficial, is a complex process that has a number of challenges in fracturing design and execution. This research focuses on studying the damage caused by the fracturing fluid (gel) to the fracture and the conditions to remove the damage. Guar gum and its derivatives have been the most commonly used polymers to increase the viscosity of fracturing fluids. The fracturing fluid gets dehydrated under pressure leaving behind a highly concentrated unbroken residue called filter cake which causes permeability impairment in the proppant pack, resulting in low fracture conductivity and decreased effective fracture length.

This study seeks to characterize filter cakes. By measuring its thickness and with the leak off volume, the concentration and yield stress of the filter cake can be estimated. The thickness of the filter cake was measured with a precise laser profilometer.

Correlations are proposed to estimate filter cake properties (thickness, concentration and yield stress) based on pumping conditions (pump rate, time and net pressure) and rock properties. With these properties known, a required flow back rate of the reservoir fluid can be estimated to clean up the filter cake modeled as a non-newtonian fluid exhibiting a yield stress.

Typical field conditions were referenced and scaled down in the lab to closely represent the field conditions. Recommendations are provided on gel damage based on the observation of the study.

## **DEDICATION**

This thesis is dedicated to my parents, Fidelis and Alice Yango, for their unwavering and selfless love, support and direction throughout my life. This thesis is also dedicated to my wife, Joy, and son, Phil, for their love and the inspiration they provide me.

## ACKNOWLEDGEMENTS

I would like to thank my committee co-chairs, Dr. Ding Zhu and Dr. Dan Hill. Their deep mastery of the subject matter, experience and insightful advice provided me with a rewarding research and learning experience. It has been a privilege working for them. My gratitude also goes to Dr. Maria Barrufet, for serving as a committee member and being very accommodating to my research needs.

Thanks also go to the department facility coordinator John Maldonado and my colleagues for their support.

I would like to thank the Harold Vance Department of Petroleum Engineering and faculty for the opportunity given me to receive a top tier education.

I also want to thank my siblings and close friends for always being there for me.

Finally, I would like to thank Schlumberger for their financial, material and technical support for this work.

## TABLE OF CONTENTS

	Page
ABSTRACT .....	iii
DEDICATION .....	v
ACKNOWLEDGEMENTS .....	vi
TABLE OF CONTENTS .....	vii
LIST OF FIGURES.....	ix
LIST OF TABLES .....	xi
1. INTRODUCTION AND LITERATURE REVIEW.....	1
1.1 Gel Damage in Hydraulic Fracturing .....	1
1.2 Literature Review .....	3
1.3 Research Objectives .....	5
2. BACKGROUND THEORY AND DESIGN OF EXPERIMENTS .....	6
2.1 Relevant Theory .....	6
2.1.1 Shear Rate and Shear Stress .....	6
2.1.2 Filter Cake Concentration .....	7
2.1.3 Filter Cake Yield Stress.....	8
2.1.4 Leak off Coefficient .....	9
2.1.5 Filter Cake Buildup and Erosion Rate.....	9
2.2 Data Collection Plan (Input Data).....	10
2.3 Experimental Test Matrix.....	11
3. EXPERIMENTAL PROCEDURE .....	14
3.1 Core Sample Preparation.....	15
3.2 Loading Cores into Conductivity Cell.....	17
3.3 Fracture Fluid Preparation.....	20
3.4 Fracture Fluid Pumping and Leak off Collection.....	23
3.5 Core Removal and Prep for Measurements.....	27
3.6 Filter Cake Thickness Measurement .....	28
3.7 Filter Cake Cleanup.....	31
4. RESULTS AND INTERPRETATION.....	33
4.1 Thickness Measurements—Profilometer Scans .....	33



	Page
4.2 Leak off Volume and Leak off Coefficient .....	34
4.2.1 Extension of Results to Conditions Not Tested .....	37
4.3 Filter Cake Thickness .....	37
4.3.1 Filter Cake Thickness Model .....	43
4.4 Filter Cake Concentration and Yield Stress .....	44
4.5 Filter Cake Characterization Workflow .....	45
4.6 Fracture Performance and Filter Cake Clean up .....	46
4.6.1 Filter Cake Effects on Fracture Performance .....	46
4.6.2 Filter Cake Cleanup.....	47
4.6.3 Other Cleanup Considerations .....	51
5. CONCLUSIONS AND RECOMMENDATIONS.....	53
5.1 Conclusions .....	53
5.2 Recommendations .....	54
NOMENCLATURE .....	56
REFERENCES .....	57
APPENDIX .....	59
VITA .....	64

## LIST OF FIGURES

	Page
Fig. 1—Filter cake on core face .....	2
Fig. 2—Filter cake volume balance schematic .....	7
Fig. 3—Filter cake buildup procedure .....	14
Fig. 4— Core surface before and after coating with silicone.....	15
Fig. 5—Core saturation vacuum pump setup.....	17
Fig. 6—Hydraulic jack used for installing cores.....	18
Fig. 7—Piston for conductivity cell .....	19
Fig. 8—Details of mounted conductivity cell and spacer bar .....	19
Fig. 9—Gel mixing equipment – Mixer (A), Rheometer (B) and Sieve (C) .....	20
Fig. 10—Lumping/fish eye effect from sprinkling fast (a) versus sprinkling slow for smoother mix (b).....	21
Fig. 11—Viscosity quality control curve to establish successful guar hydration point ...	22
Fig. 12—Gelation process: A – Linear gel. B – Crosslinked gel. C – Crosslinked gel (long delay) .....	22
Fig. 13—Fracture fluid pumping set up and leak off fluid collection.....	24
Fig. 14—Suction and discharge pump (actual) connections.....	24
Fig. 15—Fractional collector showing clear leak off fluid (water).....	26
Fig. 16—Core surface before and after washoff .....	27
Fig. 17—Profilometer components (Malagon 2006) .....	28
Fig. 18—Data measurement path along the user specified scanning area .....	29

	Page
Fig. 19—Profilometer controls input screen ( <i>after</i> run button is clicked) .....	29
Fig. 20—Vernier caliper used to verify thickness measurements.....	31
Fig. 21—Thickness profile for experiment E18 ( $t_{\text{mean}} = 0.0235'' = 0.598\text{mm}$ ).....	33
Fig. 22—Leak off information for experiment E9 with $C_w = 0.0032 \text{ ft/min}^{0.5}$ .....	34
Fig. 23—Classical laboratory leak off data (McGowen 1996) .....	35
Fig. 24—Effects of shear rate on leak off .....	35
Fig. 25—Effect of shear rate on leak off coefficient.....	36
Fig. 26—Laser and caliper thickness comparison at $60\text{s}^{-1}$ shear rate .....	38
Fig. 27—Thickness profiles at different shear rates .....	38
Fig. 28—Comparison of shear induced vs. static filter cake thickness.....	40
Fig. 29—Quadratic fit on leak off data .....	41
Fig. 30—Experimental determination of filtercake mechanical stability constant .....	42
Fig. 31—Correlations for filter cake thickness .....	43
Fig. 32—Change in concentration and yield stress with leak off .....	45
Fig. 33—Filter cake characterization workflow.....	46
Fig. 34—Fracture width loss .....	47
Fig. 35—Step flow erosion test.....	50
Fig. 36—Core surfaces after erosion test .....	51
Fig. 37—Profilometer processed data output in excel .....	62
Fig. 38—Experiment E19T top core thickness profile. $t_{\text{mean}} = 0.0163''$ .....	63
Fig. 39—Experiment E9T top core thickness profile. $t_{\text{mean}} = 0.008''$ .....	63

**LIST OF TABLES**

	Page
Table 1—Experimental data collection plan.....	10
Table 2—Sample reference data for field conditions.....	11
Table 3—Shear rate comparison.....	12
Table 4—Flux comparison.....	12
Table 5—Experimental test matrix.....	13
Table 6 —Effect of shear rate on leak off coefficient.....	36
Table 7—Experimental determination of filtercake mechanical stability constant.....	42
Table 8—Cleanup test data.....	48
Table 9—Experimental data.....	59

## 1. INTRODUCTION AND LITERATURE REVIEW

### 1.1 Gel Damage in Hydraulic Fracturing

The decline in conventional hydrocarbon reserves coupled with increased demand for hydrocarbons has challenged the industry to explore the development of unconventional reservoirs to meet the rising energy demand. Unconventional reservoirs typically have low productivities due to low permeability and must be stimulated to produce economically. The most common stimulation method in low permeability reservoirs is hydraulic fracturing. Horizontal drilling and acidizing are other methods used to improve productivity.

Hydraulic fracturing is a stimulation method in low permeability reservoirs that uses a high pressure fracturing fluid to break the target formation creating a fracture and uniformly transporting proppant to the fracture to keep it open, creating a highly conductive path. Fracturing fluid is a mixture of a base fluid (usually water), polymer (guar) and other polymer crosslinking additives to control the viscosity. Crosslinking additives increase the viscosity of the fluid which enables uniform transportation of proppant and also allows the use of lower polymer concentrations. The fracture provides improved connectivity between the reservoir and wellbore, bypasses formation damage and alters the flow path of reservoir fluids thereby increasing well productivity. This method is mostly used to improve the conductivity of unconventional reservoirs such as coalbed methane, shale gas and tight sand formations.

---

This thesis follows the style of *SPE Journal*.

Hydraulic fracturing, though greatly beneficial, is a complex process that has a number of challenges. This research focuses on addressing the issues related to hydraulic fracturing fluid gel damage. During the fracturing process, a portion of the fracturing fluid (usually the base fluid) which is pumped under pressure permeates into the rock matrix through the fracture wall. This leaves behind the polymer which concentrates on the fracture wall, forming a filter cake (Fig. 1). Polymer solids usually are larger than pore size.



**Fig. 1—Filter cake on core face**

The filter cake behaves as a non-newtonian fluid having a yield stress. If not cleaned up after fracturing, it can reduce the effective fracture half length and available width, hence reducing the conductivity of the fracture. It is important to study the characteristics of the filter cake to allow cleaning up the filter cake and optimizing the conductivity created by hydraulic fractures. With the effective clean up of fractures, production can benefit from the increased effective fracture length.

## 1.2 Literature Review

Many researchers have worked on hydraulic fracturing gel damage resulting in findings from which this research is built on, modifies or introduces methods to better capture the effects of gel damage.

McDaniel conducted experiments indicating lower fracture conductivity with a filter cake as opposed to no filter cake (McDaniel and Parker 1988). The study indicated a decrease in fracture conductivity with an increase in closure stress. The thickness of the filter cake was not measured which can allow isolating the contribution of filter cake on fracture conductivity from the effect of closure stress.

Prud'homme measured filter cake thickness as a function of gel concentration but used a membrane instead of a core sample which is not as representative of field conditions (Prud'homme and Wang 1993). However, they made a useful observation that the filter cake thickness growth is a function of the shear stress of the fracturing fluid exerted on the fracture wall and the yield stress of the filter cake that builds up. The filter cake grows when the shear stress of the fracturing fluid is lower than the yield stress of the filter cake. Growth stops when they are equal and the filter cake is eroded when the shear stress exceeds the yield stress.

Navarrete studied the effect of shear rate on the dynamic fluid loss behavior of linear gels and crosslinked borate guar in 'low' (less than 0.5 md) to 'high' permeability (70 md) rocks (Navarrete et al. 1996). This was useful in this study to characterize dynamic fluid loss behavior in a tight rock where leakoff behavior is controlled by the formation of a filter cake—the leak off rate decreases as filter cake buildup increases.

The correlations proposed for the shear rate and leakoff coefficient are discussed in subsection 2.3.1.

McGowen and Vitthal (1996) proposed benchmark information on running dynamic fluid loss experiments including fluid leak off modeling, the effect of a conductivity cell on the formation of filter cake, and the type of fracturing fluid used. The study serves as a guideline for dynamic fluid loss experiments but with focus on high permeability cores.

Ayoub et al. (2006) conducted extensive laboratory experiments on filter cake concluding that the polymer in a crosslinked guar is concentrated only in the filter cake during leakoff which is observed in this study. Based on this, they recommended that fracture placement models should calculate filter cake thickness rather than average polymer concentration. This assists in the design of treatments to avoid filter cake blockage of fracture width and provide the needed input for modeling fracture clean up considering non-Newtonian fluids exhibiting a yield stress.

Xu et al. (2011) used a slotted plate method to directly measure the yield stress of a crosslinked guar polymer gel with and without a breaker. The yield stress was measured for polymer concentrations ranging from 40 lb/Mgal to 200 lb/Mgal. This information is used in this study to estimate the yield stress of filter cake.

Finally, Xu et al (2011) measured filter cake thickness under static leak off conditions. Instead of pumping a gel while leaking off, the gel was placed in a closed conductivity cell and then pressure was applied to engender leak off. This study offers an



improvement by leaking off while pumping gel to create a filter cake which is a better representation of what happens in the field.

### **1.3 Research Objectives**

This research is aimed at characterizing the buildup of filter cake under dynamic fluid loss conditions. Correlations are proposed to estimate filter cake properties, including thickness, concentration and yield stress. These properties are used as an input to a theoretical model that can estimate the flow back rate required to clean up the filter cake. Experiments are run to verify the model. The goals are outlined below.

1. Design and set up an experimental apparatus and procedures used to pump hydraulic fracturing gel through a conductivity cell under pressure while allowing leak off.
2. Measure the thickness of the resulting filter cake using a laser profilometer.
3. Model filter cake buildup and its related characteristics (thickness, concentration and yield stress).
4. Design and run experiments to verify the filter cake clean up model.

## 2. BACKGROUND THEORY AND DESIGN OF EXPERIMENTS

In order to characterize the buildup of filter cake under dynamic leak off conditions and study the cleanup process, the relevant theory is discussed, a data collection plan is established and a testing matrix is presented in this section.

### 2.1 Relevant Theory

#### 2.1.1 Shear Rate and Shear Stress

To understand the gel damage problem, the first step is determining the shear rate of the pumped gel. R.C. Navarrete (Navarrete et al. 1996) proposed the following correlation for a power law fluid that relates the shear rate on the fracture or filter cake walls ( $\gamma_w$ ), the fluid flow rate ( $q$ ), the flow behavior index ( $n'$ ) and the fracture dimensions (width,  $w$  and height,  $h$ ).

$$\gamma_w = \frac{q(4+\frac{2}{n'})}{w^2h} \quad (2.1)$$

The resulting shear stress, for a Herschel-Bulkey fluid, a power law fluid with a yield stress (Economides et al. 2003), is given by

$$\tau_w = \tau_o + 47.88K'\gamma_w^n \quad (2.2)$$

where  $K'$  is the consistency index and  $\tau_o$  is the yield stress of the pumped gel. The constant in Eq. 2.2 (47.88) is the conversion factor from  $\text{Lb/ft}^2$  to Pa.

### 2.1.2 Filter Cake Concentration

The filter cake concentration is required to estimate the yield stress of the filter cake. The concentration of filter cake cannot be directly measured. Hence, a simple concentration (material) balance is used to estimate the concentration of the filter cake. It is assumed here that the compressibility of the filtrate (water) is negligible so that the leak off volume collected has an equivalent volume under the 500 psi pressure during leak off. It is also assumed that no polymer (solids) is in the filtrate and is left behind as a residue to build up filter cake. It was verified in the experiments that only the base fluid (water) was filtered as shown in Fig. 2. Also, the equations are valid for a static buildup, i.e. no erosion of filter cake.

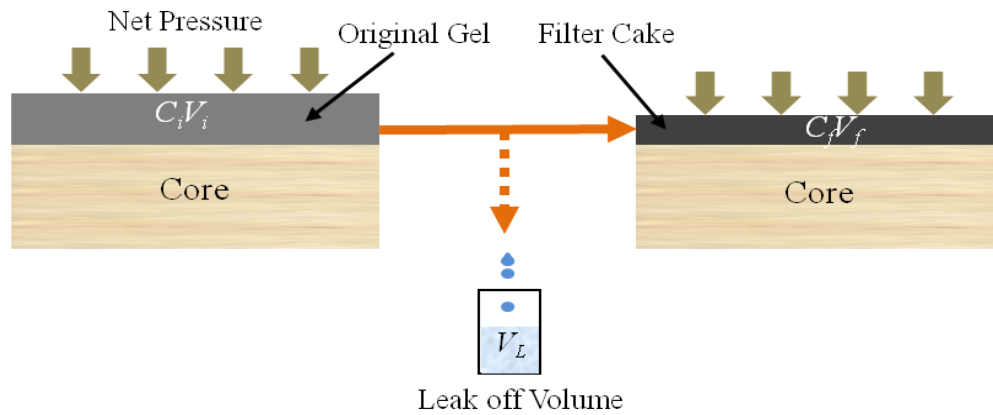


**Fig. 2—Filter cake volume balance schematic**

The filter cake concentration balance is given by

$$C_i V_i = C_{FC} V_{FC} \quad (2.3)$$

where  $C_i$  is the original gel concentration and  $C_{FC}$  is the filter cake concentration. The initial volume ( $V_i$ ) is the sum of the filter cake volume ( $V_{FC}$ ) and leak off volume ( $V_L$ )

$$V_i = V_{FC} + V_L \quad (2.4)$$

and

$$V_{FC} = t_{FC}A \quad (2.5)$$

thus

$$C_{FC} = C_i F_{CF} \quad (2.6)$$

where the filter cake concentration factor ( $F_{CF}$ ) is

$$F_{CF} = V_i / V_{FC} \quad (2.7)$$

Note:  $A$ , is the leak off cross sectional area. The core in this work has curved edges with a radius of 0.805 in. which is half the width of the core.

### ***2.1.3 Filter Cake Yield Stress***

The filter cake yield stress is required to design the cleanup requirements for the filter cake. When the shear stress of the fluid pumped through the fracture exceeds the filter cake yield stress, the filter cake is eroded (see sub section 2.1.5). With the concentration of the filter cake ( $C_{FC}$ ) known, the filter cake yield stress can be estimated. Wang experimentally determined the yield stress of guar polymer as a function of gel concentrations ranging from 40 to 200 lb/Mgal (Xu et al. 2011). The data was used in this work in two ways. For concentrations between 40 to 200 lb/Mgal, a linear interpolation was done using the closest data points. At higher filter cake concentrations, a linear regression from Wang's data is used as shown in Eq. 2.8.

$$\tau_{y_{FC}} = 0.4256C_{FC} - 21.8758 \quad (2.8)$$

### 2.1.4 Leak off Coefficient

The leak off coefficient of the rock is required to characterize leak off behavior. A fraction collector collects leak off volume in several timed test tubes. To obtain the leak off coefficient,  $C_w$ , the cumulative volume ( $V_L$ ) vs. the square root of time is plotted. In early time, the leak off rate is high as the filtrate displaces the formation or rock fluid before a filter cake is formed. This is called spurt loss. After spurt, the deposition of filter cake begins which controls the leak off rate (reduces amount of leak off). In late time the plot exhibits a linear trend with a slope,  $m \left( \frac{V_L}{\sqrt{t}} \right)$ , which is used to calculate the leak off coefficient as shown in Eq. 2.9.

$$C_w = \frac{1}{12} \cdot \frac{V_L}{2A\sqrt{t}} \quad (2.9)$$

where A is the total leak off surface area and 1/12 is the conversion factor from in. to ft.

### 2.1.5 Filter Cake Buildup and Erosion Rate

The shear rate of the pumped gel affects the filter cake growth rate. This can be quantified using correlations (Eq. 2.10) proposed by Prud'homme. (Prud'homme and Wang 1993).

$$\begin{aligned} \frac{dM}{dt} &= \omega U, \quad \tau_w < \tau_{yFC} \\ &= 0, \quad \tau_w = \tau_{yFC} \\ &= \text{rate of erosion}, \quad \tau_w > \tau_{yFC} \end{aligned} \quad (2.10)$$

where  $\omega$  is the mass fraction of solids in the fluid phase, M is the mass/area of the filter cake and U is the solvent velocity through the filter cake.

If the shear stress of the pumped fluid exceeds the yield stress of the filter cake, then the filter cake is eroded with time. If the shear stress is less, then the filter cake grows with time. The buildup and erosion rates are defined by Eq. 2.10.

## 2.2 Data Collection Plan (Input Data)

To effectively characterize the buildup and cleanup of filter cake, a wide range of data needs to be collected to ensure quality control for the experiments and provide inputs for theoretical or empirical correlations discussed in section 2.1. The details of each quantity is illustrated in Table 1.

**Table 1—Experimental data collection plan**

Quantity	Instrument	Purpose
Temperature	Infra red temperature gun	Quality control on linear gel viscosity
	Inline thermocouple	Calculate rheological properties ( $n'$ , $K'$ )
Pressure	Mechanical pressure gauges	Determine and monitor leak off pressure (controlled with a back pressure valve)
Flow rate	Stop watch, graduated cup*	Used to calculate gel shear rate
Leak off volume	Fractional collector	Used to calculate filter cake concentration
Leak off rate		Used to calculate leak off coefficient
Filter cake thickness	Laser profilometer	3D surface measurements of filter cake
	Vernier caliper	Back up or control on laser measurements
Viscosity	Rheometer	Quality control on linear gel viscosity
pH	pH meter	Quality control on crosslinked gel

\* Due to the extremely high viscosity of the crosslinked gel (in excess of 5,000 cp), conventional digital flow meters could not be used in the lab. A stop watch and a graduated vessel are commonly used to calibrate flow meters. Also, a positive displacement pump was used for these experiments with a constant back pressure which kept flow rates stable.

### 2.3 Experimental Test Matrix

One goal of this research is to, at a lab scale, simulate pumping hydraulic fracturing gel and studying the buildup and clean up of filter cake.

For high viscosity fracture fluids with a gel concentration of 40lb/Mgal, typical field pumping rates are 20 – 40 bpm usually lasting anywhere from 1 hour to 3 hours with a fracture height of 100 – 300 ft. The cores used for the experiments were from a Kentucky sandstone with permeability in the range of 0.1–1.0 md to represent a tight gas sandstone. The experiments were conducted to closely mimic the resulting field shear rate or flux as much as the capability of lab equipment allowed. A data summary is illustrated in Tables 2, 3 and 4.

**Table 2—Sample reference data for field conditions**

Temp	175 °F
Flow rate	20 bpm
Fracture width, $w$	0.250 in
Fracture height, $h$	300 ft
Cross sectional area, $A$	900 in <sup>2</sup>
Flow behavior index, $n'$	0.4340
Consistency index, $K'$	0.0990 lbf-s <sup><math>n'</math></sup> /ft <sup>2</sup>
Flux	19.7 ft/min
Shear rate	123.73 s <sup>-1</sup>

**Table 3—Shear rate comparison**

Pump Rate Bpm	Fracture Height		
	100ft	200ft	300ft
	Shear Rate s <sup>-1</sup>		
5	92.8	46.4	30.9
10	185.6	92.8	61.9
20	371.2	185.6	123.7
30	556.8	278.4	185.6
40	742.4	371.2	247.5

The green shaded cells represent the shear rates that are closely matched in the experiments. Several experiments are conducted to establish trends that allow extension of the results to higher shear rates. The corresponding flux for the experiments is in the range of 0.07 – 0.4 ft/s with details summarized in Table 4.

**Table 4—Flux comparison**

Pump Rate Bpm	Fracture Height		
	100ft	200ft	300ft
	Gel Flux in Fracture ft/s		
5	0.225	0.1125	0.1
10	0.45	0.225	0.2
30	1.35	0.675	0.5
40	1.8	0.9	0.6

To closely capture field conditions, the test matrix illustrated in Table 5 is implemented. For all experiments the gel is crosslinked at room temperature without compromising gel composition. Note that at higher temperatures, a higher pH is needed to maintain the same crosslinking specie concentration (borate anion vs. boric acid).



**Table 5—Experimental test matrix**

<b>Fracture Width (in.)</b>	<b>0.25</b>											
<b>Shear Rate (s<sup>-1</sup>)</b>	<b>20</b>				<b>60</b>				<b>100</b>			
<b>Leakoff Time (min.)</b>	<b>60</b>	<b>90</b>	<b>120</b>	<b>150</b>	<b>60</b>	<b>90</b>	<b>120</b>	<b>150</b>	<b>60</b>	<b>90</b>	<b>120</b>	<b>150</b>

Some experiments were repeated to validate the trends established by the test matrix.

### 3. EXPERIMENTAL PROCEDURE

The primary purpose of this study was to build up filter cake under dynamic leak off conditions, measure the resulting filter cake thickness and also run cleanup experiments based on a model developed to characterize the filter cake.

In order to characterize the filter cake surface to closely represent field conditions, the experiments were run based on the test matrix shown in sub section 2.3. Note that the experiments were done at room temperature to ease the fracture fluid crosslinking process.

The following general procedure (Fig. 3) was used for the dynamic buildup experiments (some clean up experiments were performed after buildup).

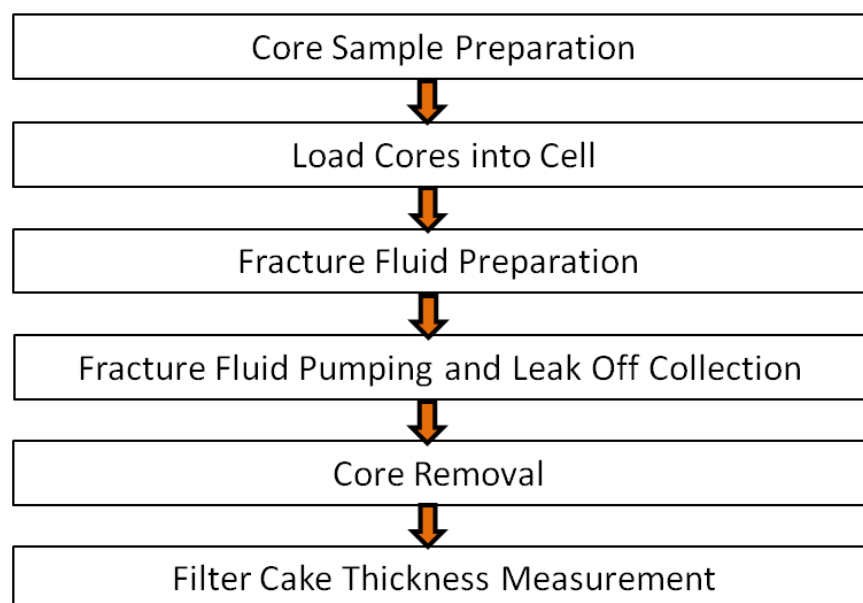


**Fig. 3—Filter cake buildup procedure**

### 3.1 Core Sample Preparation

The core samples used for this experiment were from a Kentucky sandstone with permeability ranging from 0.1 – 1.5 md and porosity from 11-14%. The cut cores measured 7in. long by 1.61in. wide by 3 in. tall. The cores are coated with silicone to provide a primary seal between the core and the conductivity cell through a tight fit. A secondary and essential seal is provided through a combination of Teflon tape, vacuum grease and an O ring and will be discussed in sub section 3.2. Fig. 4 illustrates the before and after coated core. Notice the chamfered edge on the core silicone edge to prevent knocking out the O ring.

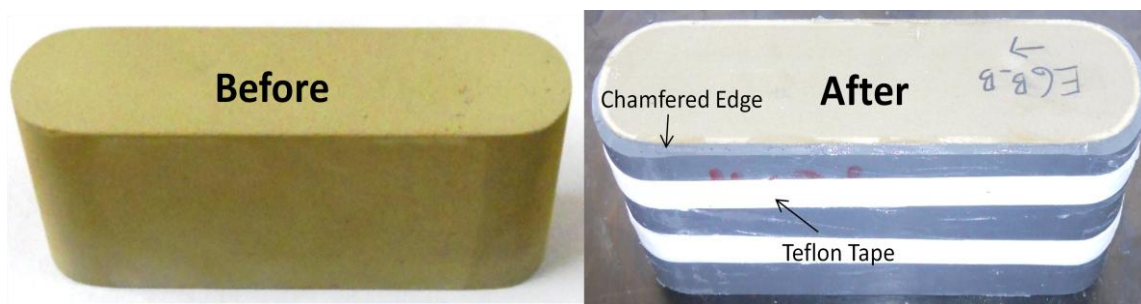


**Fig. 4— Core surface before and after coating with silicone**

The core samples are prepared using the following standard procedure:

1. Prepare and clean the rock samples that need to be molded.
2. Put 3M blue painters tape on the top and bottom of the core sample, cutting the edges with a razor cutter.
3. Apply silicone primer (SS415501P), about three times with a brush, along the edges of the core samples. Allow 15 minutes waiting time in between primer

applications.

4. The mold is made of stainless steel, with a plastic bottom. Clean the metal surface and bottom plastic piece of the mold with acetone using a cloth.
5. Spray silicon mold release S00315 on the metal molds three (3) times. Wait for two (2) minutes between each spray.
6. Assemble the mold. Tighten the four bolts at the bottom and the three bolts on the side. Make sure all bolts are tight.
7. Put the rock in the mold and adjust to center position.
8. Prepare 75cc of silicone potting compound and 75cc of silicon curing agent from the RTV 627 022 kit for a 1:1 mixing ratio. Weigh before mixing both components to ensure that the mixture is 50/50 of each component, either by volume or by weight percent. Mix and stir thoroughly.
9. With a disposal beaker pour the mixture in the gap between the core and the mold carefully until the silicone fills to the top of the core sample.
10. Let mold set for 24 hours in an area of at least room temperature. *To accelerate the curing process, the mold can be put in an oven at 60 °C for at least 3 hours*
11. Unscrew all the bolts from the mold and carefully remove the samples from the mold using a c-clamp.
12. Cut extra silicon on the edges with a razor cutter.
13. Remove blue painters tape from core surfaces.
14. Label the rock sample. The core sample is ready to use.
15. The core samples are initially saturated with air. Prior to

running an experiment, the core samples are saturated with the base fluid (usually water) using the vacuum pump and bowl as shown in Fig. 5. The procedure

to do this is as follows:

- a. Clean the beaker to remove any old fluid and solids.
- b. Fill the beaker with 2.5 L of base fluid
- c. Place the clean core samples in the beaker. *The core samples must be fully submerged.*
- d. Apply vacuum grease along the rim of the beaker and press the lid down. *Make sure the lid is sealed.*
- e. Turn on the pump. *Check to see if bubbles are coming out of the core sample indicating that the air is sucked out. Run this pump for about 3 hours.*



**Fig. 5—Core saturation vacuum pump setup**

### **3.2 Loading Cores into Conductivity Cell**

The saturated cores are loaded into a modified API RP-61 conductivity cell with dimensions of 10 in. long by 3-1/4 in. wide by 8 in. tall. A tight fit exists between the

coated cores and the API cell, hence a hydraulic jack (Fig. 6) must be used to push the cores in slowly. Before loading the cores, an O ring must be secured in the O ring groove of the cell. This provides a good seal capable of withstanding pumping pressures in excess of 500psi. Ensure the chamfered edge (Fig. 4) of the core goes in first. This helps snap the O ring into the groove during core placement. Leave a gap of about  $\frac{3}{4}$  inches between the top and bottom core faces – this is later reduced to the desired fracture width on the load frame.

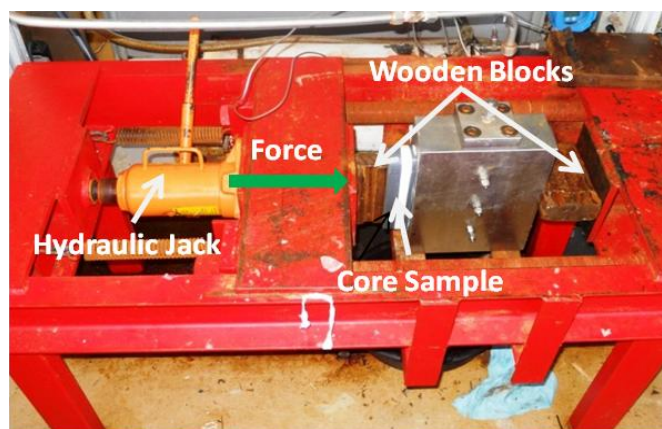


**Fig. 6—Hydraulic jack used for installing cores**

There are two 3 in. tall pistons that are installed after the cores are in place. The pistons are used to keep the cores in place while the cell is under pressure and each have a viton polypack seal to prevent leaking of leak off fluid through the cell body. Instead, the pistons have milled channels that convey leak off fluid through a pilot hole to a leak off connection as shown in Fig. 7.

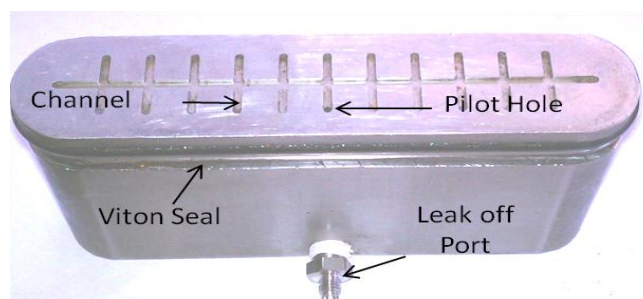


**Fig. 7—Piston for conductivity cell**

A hydraulic load frame is used to adjust the gap between the core faces to the required fracture width. Ensure the top and bottom pistons are level before applying pressure. The desired fracture width for this work is  $\frac{1}{4}$  in. Hence, a  $\frac{1}{4}$  in. spacer bar is placed between the core faces and inserted no deeper than 1 in. to allow easy removal (Fig. 8). Pressure is applied slowly till the bar is just snug. At this point, the spacer bar is removed and fracture width is confirmed with a triangular edged ruler. Check the entry and outlet and adjust the width as necessary, making sure the supply pressure to the load frame is extremely small (less than 10 psi) to allow very fine movements.

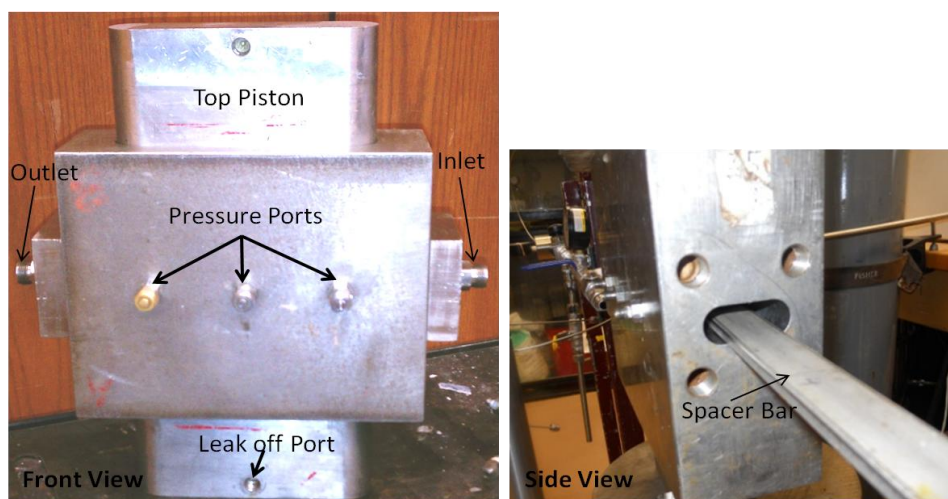


**Fig. 8—Details of mounted conductivity cell and spacer bar**

### 3.3 Fracture Fluid Preparation

A borate crosslinked guar is used as the fracturing fluid for this research. The guar polymer is mixed at a concentration of 40 Lb/Mgal, a common concentration used in industry for high viscosity fracturing. The gel is mixed at room temperature to facilitate mixing without compromising crosslinked gel properties. A higher pH is needed at higher temperature to maintain the same crosslinking specie concentration (borate anion vs. boric acid). To prepare the fluid, the following are required (Fig. 9):

- A fine mesh sieve
- A Rheometer (Fann 35 Multispeed Rheometer)
- A mixer (Carfamo Stirrer Type RZR50, 100W)
- Graduated syringes
- Chemicals: Guar Polymer, Boric Acid, Sodium Hydroxide, Potassium Chloride

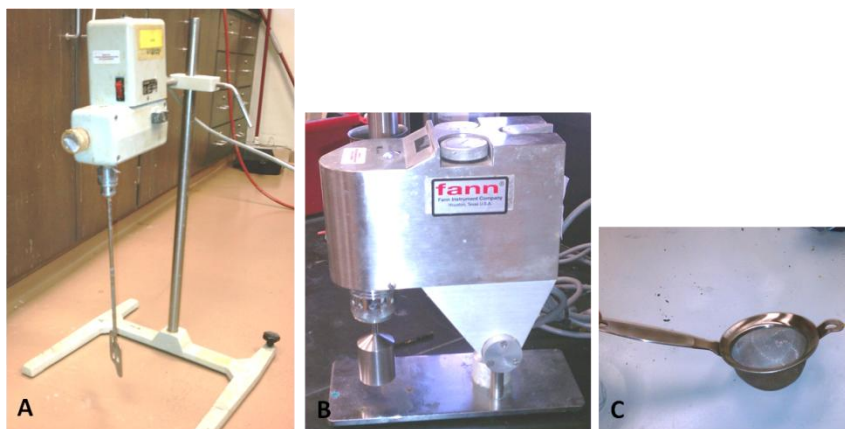


**Fig. 9—Gel mixing equipment – Mixer (A), Rheometer (B) and Sieve (C)**



Schlumberger provided the chemicals and mixing procedure. The mixing procedure was modified to suit this work as follows:

1. First hydrate the guar. This is often done in the presence of KCl. Mix KCl with water and stir to dissolve. Adjust the speed of the mixer to get a vortex that does not extend all the way down to the bottom of the tank. The vortex bottom should be 50 to 80% of the distance to the bottom. Add the guar by sprinkling it onto the shoulder of the vortex very slowly to avoid lumping and fisheyes (Fig. 10). With time, the size of the vortex reduces as the fluid viscosifies.

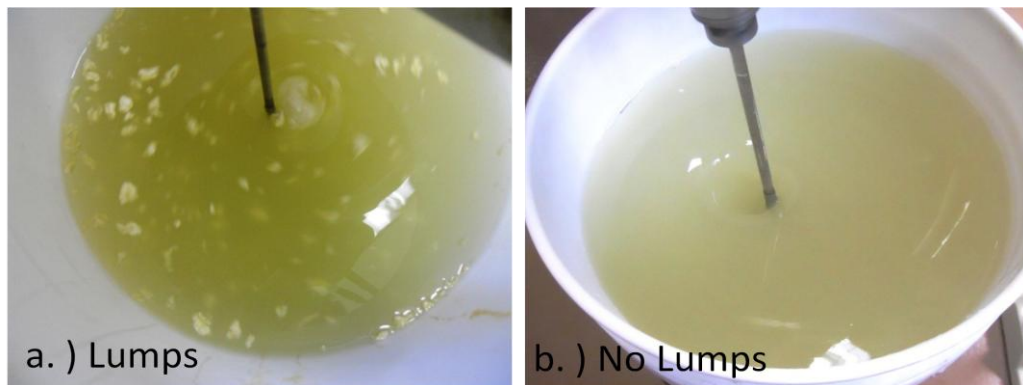


**Fig. 10—Lumping/fish eye effect from sprinkling fast (a) versus sprinkling slow for smoother mix (b)**

2. The guar should mix 15 to 25 minutes to fully hydrate. The successful hydration point can be assessed by measuring the viscosity on a Fann35 rheometer at a shear rate of  $511 \text{ s}^{-1}$  (300 rpm). See Fig. 11 for reference.

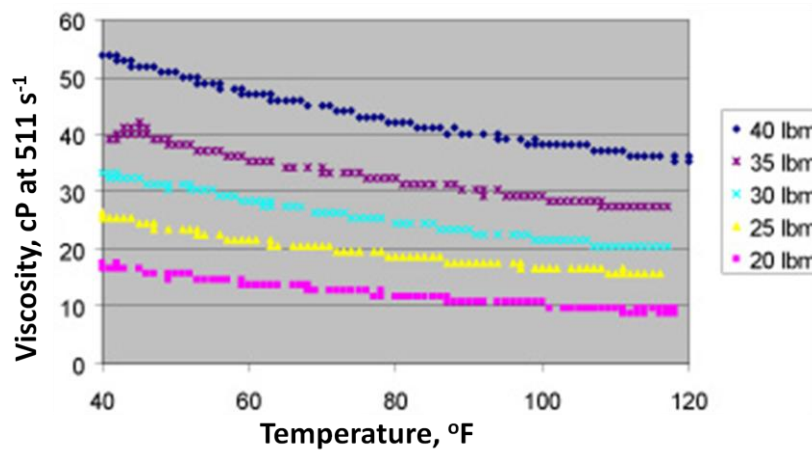


**Fig. 11—Viscosity quality control curve to establish successful guar hydration point**

3. Add the diluted solution of boric acid while stirring. Stir for 2 minutes.
4. Add in the breaker if used. Stir for 1 minute.
5. Increase the mixing speed and add the caustic solution quickly. The fluid should gel almost immediately (Fig. 12).

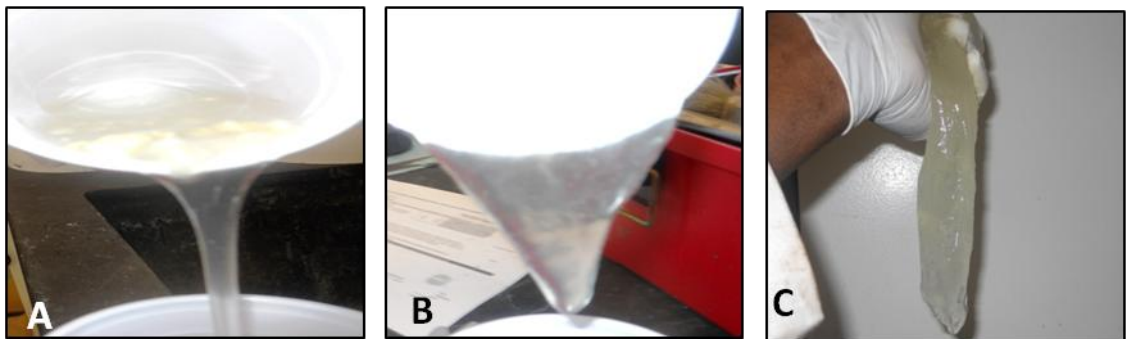


**Fig. 12—Gelation process: A – Linear gel. B – Crosslinked gel. C – Crosslinked gel (long delay)**

6. The pH can be measured. It should be at least 8.5 but no more than 12. Higher pH is needed at higher temperature to maintain the same crosslinking specie

concentration (borate anion vs. boric acid). Higher temperature shifts the equilibrium towards boric acid. A pH of 9-11 is OK for ambient gels.

Note: If the pH is too high, DO NOT add boric acid to reduce the pH. If this happens, dispose of the fluid and start over.

### **3.4 Fracture Fluid Pumping and Leak off Collection**

After the fracturing fluid is mixed, it is pumped at varying rates (Table 5) under pressure through the cell where leak off fluid is collected and a filter cake residue builds on the two rock faces installed per sub section 3.2. Sub section 3.7 describes the procedure to clean up filter cake. The following set of equipment is used for the filter cake build up experiments (Fig. 13).

- Building air compressor supply
- Backup compressor for high shear rate experiments
- Supply tank and waste tank
- Suction supply pump (Yamada NDP-20BPS-PP diaphragm pump)
- High pressure discharge pump (Hydracell diaphragm pump, D10IKCTHFECA)
- Pressure relief valve (Warner C22ABSVRREF)
- Modified API RP-61 conductivity cell
- Load frame
- Liquid fractional collector (Gilson FC 203B)
- Back pressure valve (MITY MITE S-90W, 10 – 2000psi)
- Isolation valves (Swagelok SS-AFSS8)

- Pressure gauges

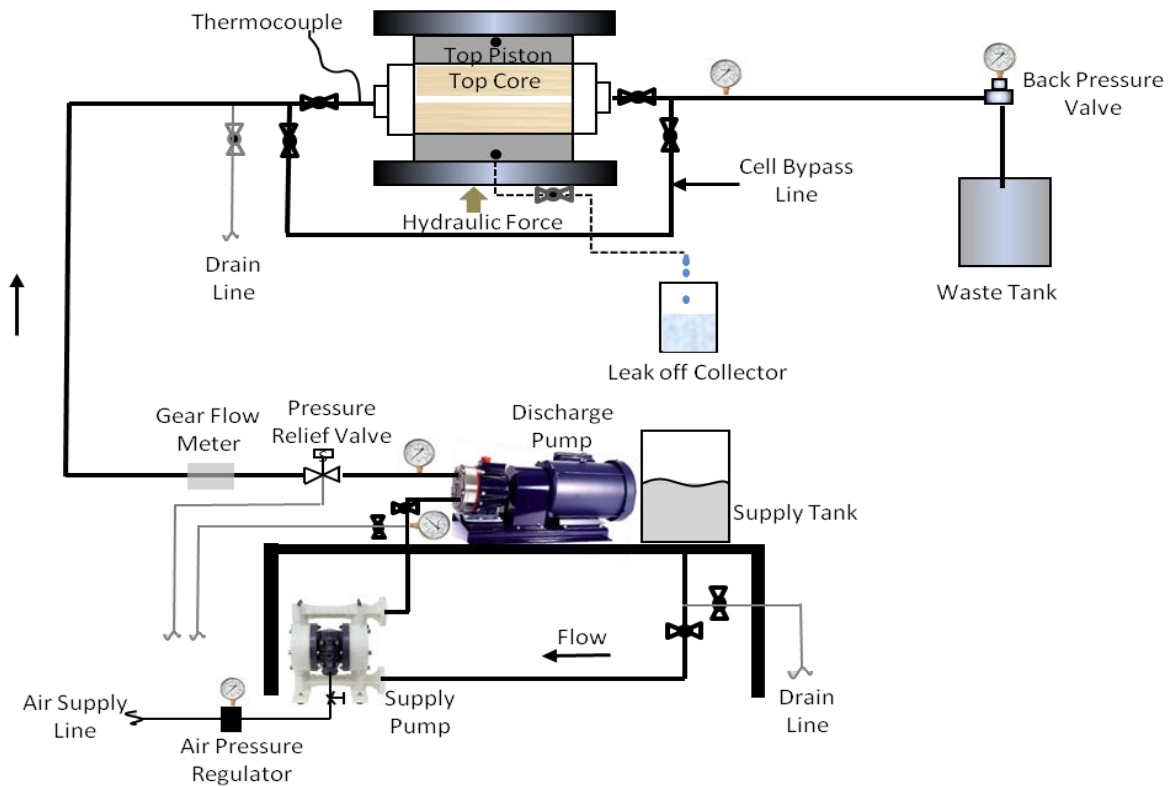


**Fig. 13—Fracture fluid pumping set up and leak off fluid collection**

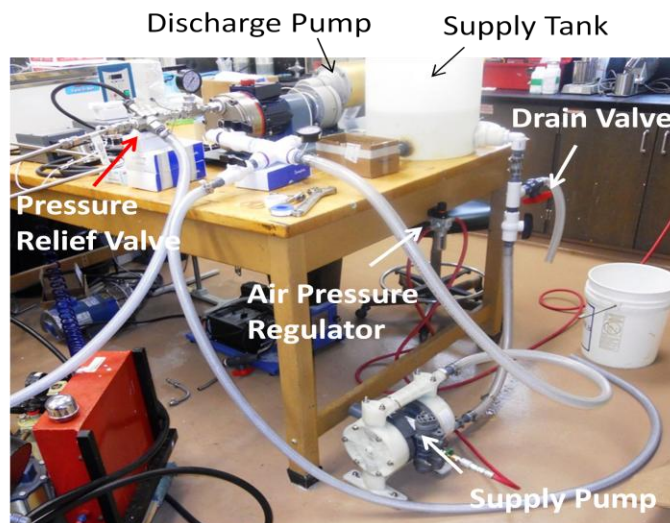


**Fig. 14—Suction and discharge pump (actual) connections**

Once the fluid is mixed, it is transferred to the 10 gallon supply tank. The required mix volumes depend on the pumping rate and pumping time. The isolation valves are opened or closed to allow flow of fracture fluid in the direction indicated by the flow arrows in Fig. 13. Using the air pressure regulator, the air supply pressure to the diaphragm supply pump is set between 20 – 70 psi depending on required flow rate (higher flow rates will require higher pressures).

Note: For the high rate experiments ( $100 \text{ s}^{-1}$ ), the air supply requirements of the Yamada supply pump go up – in excess of 30 SCFM at 60 - 70 psi. The building compressor supplies about 18SCFM, so an additional compressor with a capacity of 10 SCFM was rented and plumbed in parallel with the building air supply to provide additional flow at the same pressure. Check valves must be used to prevent back flow.

The diaphragm supply pump is turned on by opening the valve to its air supply inlet. While the supply pump discharge line is empty or if an undesired fluid is in the discharge line, use the Hydracell discharge pump bypass valve. Once the discharge line is purged by the desired fluid, close the discharge pump bypass valve and open the valve to the inlet of the Hydracell discharge pump and immediately turn on the pump. Set the discharge pump speed based on the desired pump rate. The supply and discharge pump are synchronized by monitoring the discharge pressure of the supply pump – this should not exceed 60 psi. The Hydracell discharge pump is capable of a 1000psi discharge pressure. To protect the pump, a relief is installed downstream of the pump and is set to 700 psi. The desired pressure for this work is 500 psi which is achieved by pressuring the dome of the back pressure valve to 500 psi with air. The cell bypass line is used to

check the rate (and also to flush the line after experiments when the cell is taken out). Once the pressure and rate are set, fluid is pumped through the cell and within 3 minutes, the leak off valves of the top and bottom pistons (Fig. 13) are opened and the fractional collector started. If a one sided test is needed, only one leak off port needs to be opened. All build up experiments were two sided to better represent field conditions. The fractional collector is set to sample at a rate of 30 seconds to 2 minutes per tube depending on pumping rate. With the gel under pressure, the base fluid (water) is filtered through the rock and collected through the leak off fractional collector. Ensure only water is present in the leak off tubes as shown in Fig. 15. If any gel is present, then that indicates a broken seal and the experiment must be stopped, the cell is taken apart and the seal and cores are replaced.



**Fig. 15—Fractional collector showing clear leak off fluid (water)**

As leak off volume increases, the gel gets dehydrated leaving behind the residue called filter cake. After the desired pumping time, the fractional collector is stopped as well as all pumps. The core removal procedure is described in sub section 3.5 below.

### 3.5 Core Removal and Prep for Measurements

After pumping is completed as described in sub section 3.4, the drain valve upstream of the cell is opened to relieve pressure from the cell. The inlet and outlet tube connections of the cell are quickly replaced with caps to prevent gel outflow. Since the gel is hard to flow, very little gel, if any, flows out after the line pressure is released. Filter cake builds up on core faces while gel remains in the rest of the fracture space. It is important to keep most of the gel in place to prevent filter cake contact between the top and bottom core during removal since the core is removed with pressure from one end. The top and bottom pistons are taken out and the cell, with the inlet and outlet capped, is loaded on the hydraulic jack frame that was used to install the cores (Fig. 6). Wooden blocks are aligned with the cores and used to push out the cores. Before the first core is out, it must be supported from the bottom to prevent it from dropping and possibly damaging the filter cake. The gel between the filter cake surfaces allows for easy separation between the top and bottom cores. A little cut at the center may be required sometimes to dislodge the outer core. The core face will have excess gel that must be washed off gently leaving filter cake. Fig. 16 illustrates the core surface before and after wash off.

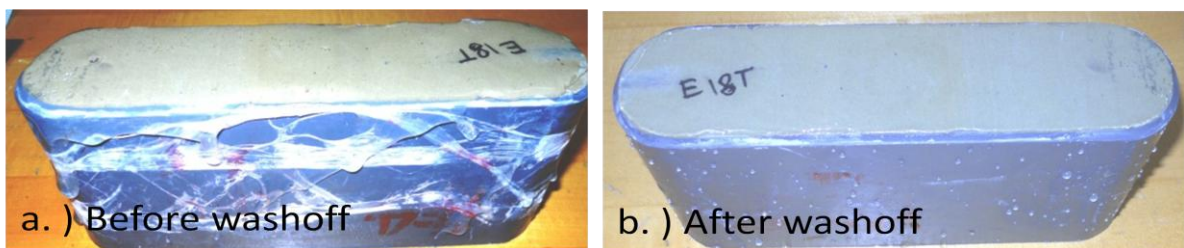


**Fig. 16—Core surface before and after washoff**

Note: The excess gel on the cores should only be washed off once the laser profilometer for thickness measurements has been completely set and ready to take measurements. This is to prevent some of the water from the filter cake evaporating while the laser equipment is set up.

### 3.6 Filter Cake Thickness Measurement

A laser profilometer is used to measure the thickness profile of the filter cake. After the excess gel is washed off, the core is placed on the servo table of the laser profilometer (Fig. 17). Remember to wash off excess gel only after the profilometer has been set up.

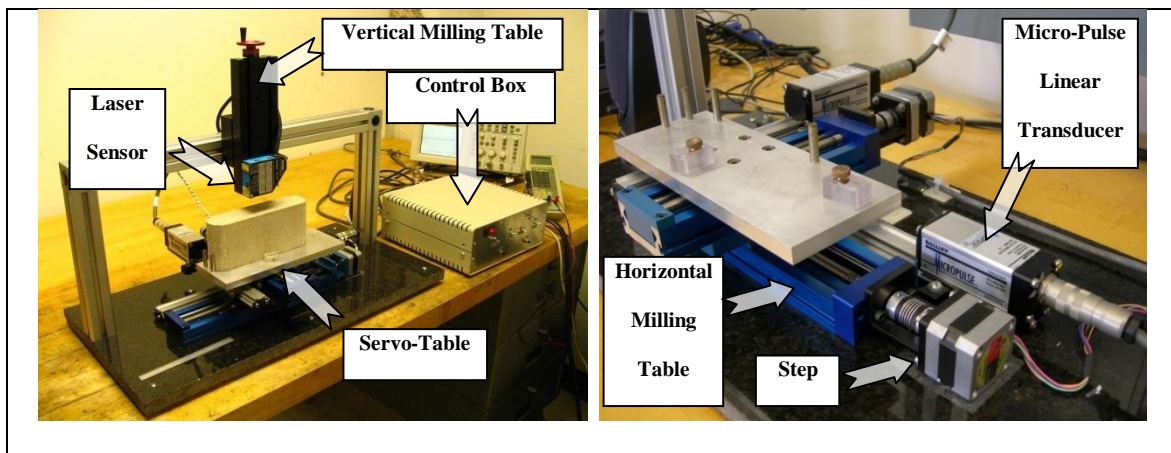


**Fig. 17—Profilometer components (Malagon 2006)**

The profilometer is designed to have a two axis (X and Y) movement in the horizontal plane while the laser captures surface depth in the vertical (z) plane. In the XY plane, the laser moves back and forth in a pattern as shown in Fig. 18. The y-



direction ‘jumps’ are determined by a user entered resolution. The resolution also determines the spacing between each data point in the laser pattern.

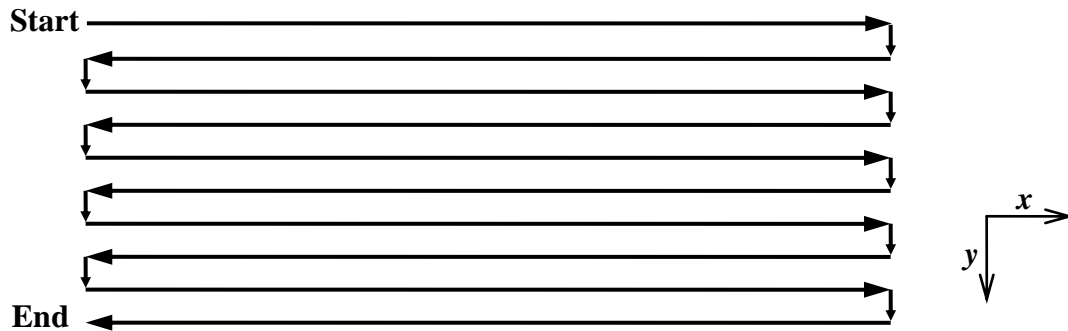



**Fig. 18—Data measurement path along the user specified scanning area**

To set up the laser, the following procedure is followed after the core is placed on the servo table and secured using the table screws

- 1.) First turn on the profilometer control box (switch is on box)
- 2.) Open the labview program **profilomenter.vi** (Fig. 19)

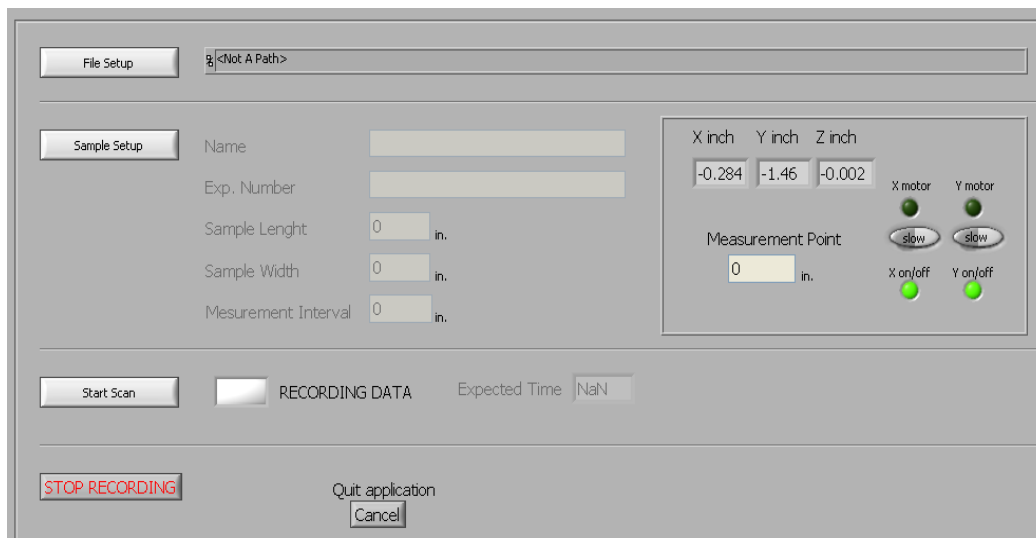



**Fig. 19—Profilometer controls input screen (after run button is clicked)**

- 3.) Hit the run button ()
- 4.) Put the mode switches on the profilometer control box to manual and jog using the position buttons so that the X inch and Y inch coordinates are zero inches. You do not need to adjust the Z position, it is read in from the laser – unless the laser is out of range.
- 5.) Click on **File Setup** then enter file name and location
- 6.) Click on **Sample Setup** and enter sample name, experiment number, sample length and measurement interval.

It is recommended to use a measurement interval no smaller than 0.1 in. to allow faster scanning. This prevents evaporation of water if the filter cake is exposed for too long. An interval of 0.2 in. was used without compromising results accuracy especially as the filter cake surface was fairly uniform. The sample length used was 7 in. and the sample width 1.7 in.

- 7.) Set the X motor and Y motor by clicking on the toggle button “**slow**”
- 8.) Put the switches on the laser control box to Auto and click on **Start Scan**
- 9.) Once recording is finished click on STOP RECORDING then click on the abort

execution button () . The scanned file (\*.dat) should now be saved in the user specified location. The file is in ASCII format and contains the XYZ coordinates of the filter cake surface.

10.) Without removing the core from the servo table, scrape off the filter cake using a flat head knife which is at least as wide as the filter cake. Removing the core from the profilometer can affect the thickness reference. Repeat steps 2 to 9.

A VBA code was programmed to read the 3D data and order it in matrix format for display in a spreadsheet which allows plotting a 3D surface using Microsoft Excel's surface plot feature. The data and plots are used to calculate a mean filter cake thickness and analyze the surface of the filter cake. Details of the VBA code and instructions on how to process the data in Microsoft Excel are outlined in Appendix A-2.

Back up measurements are taken at 8 points around the filter cake surface with a digital Vernier Caliper at a  $\pm 0.0001$  in. resolution (Fig. 20). The readings are taken before the core is placed on the profilometer and after scanning is complete. The mean thickness readings agreed closely with the laser's (Fig. 26).

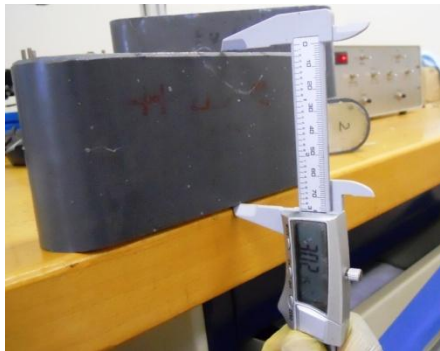


**Fig. 20—Vernier caliper used to verify thickness measurements**

### **3.7 Filter Cake Cleanup**

After running several build up experiments, a model was established to estimate filter cake thickness and yield stress based on leak off volume and other properties. As a

result, build up experiments can be run under specific conditions after which the clean up experiment is done without having to take measurements for the build up phase other than leak off volume. The same set up is used as in the buildup experiments, except instead of pumping gel, water is pumped. With an estimated yield stress of the filter cake based on leak off volume under specified experiment conditions, the required flow rate for the eroding fluid can be determined. The idea is that this flow (shear) rate gives rise to a shear stress and if the shear stress exceeds the yield stress of the filter cake, then the filter cake is eroded. The details of the theory are as discussed in sub section 2.1.5 and results in section 4.6.

#### 4. RESULTS AND INTERPRETATION

All experiments were run at room temperature with a 40 lb/Mgal gel pumped at a 500 psi pressure at varying shear rates and pump times using two cores through which leak off fluid is collected. The conditions and setup are described in detail in sections 2 and 3. The results obtained are discussed in this section. Additional data and information is available in Appendix A.

##### 4.1 Thickness Measurements—Profilometer Scans

A laser profilometer was used to scan each core face after a filter cake buildup as described in Section 3.6. An example of plot showing data from which the mean thickness is obtained is shown in Fig. 21.

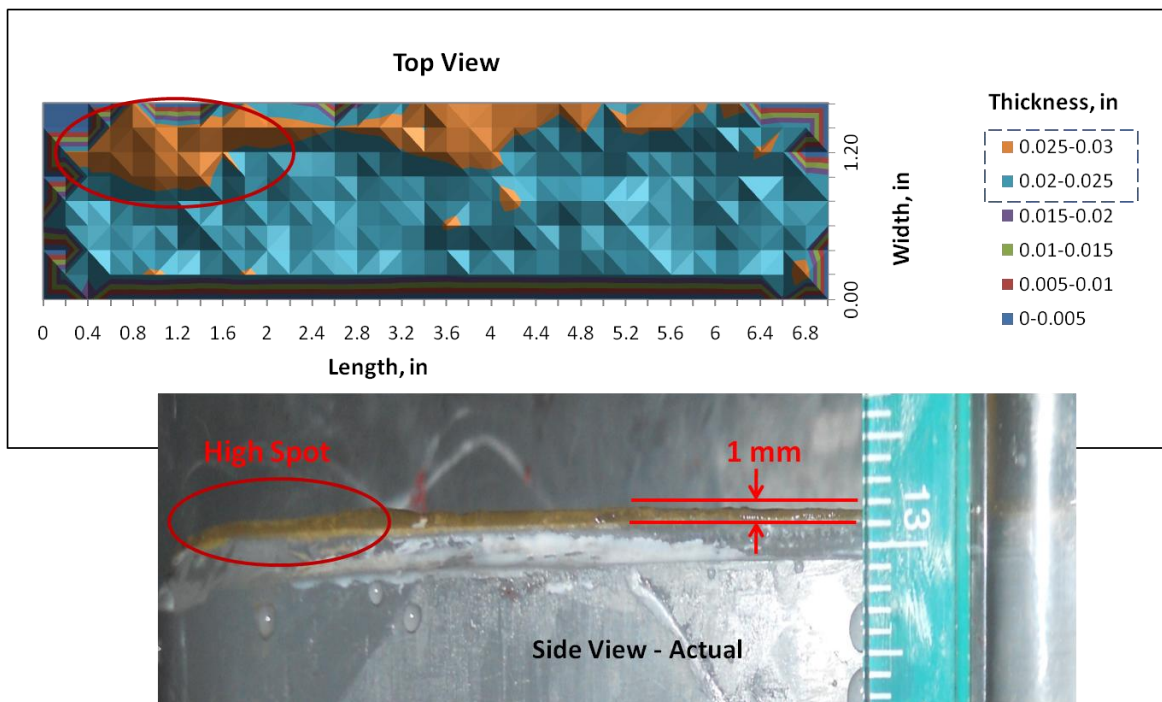


**Fig. 21—Thickness profile for experiment E18 ( $t_{\text{mean}} = 0.0235'' = 0.598\text{mm}$ )**

#### 4.2 Leak off Volume and Leak off Coefficient

The leak off volume is collected from a fractional collector which has timed test tubes. The cumulative leak off volume is plotted against the square root of time and using the slope in late time, the leak off coefficient is obtained as described in sub section 2.1.4.

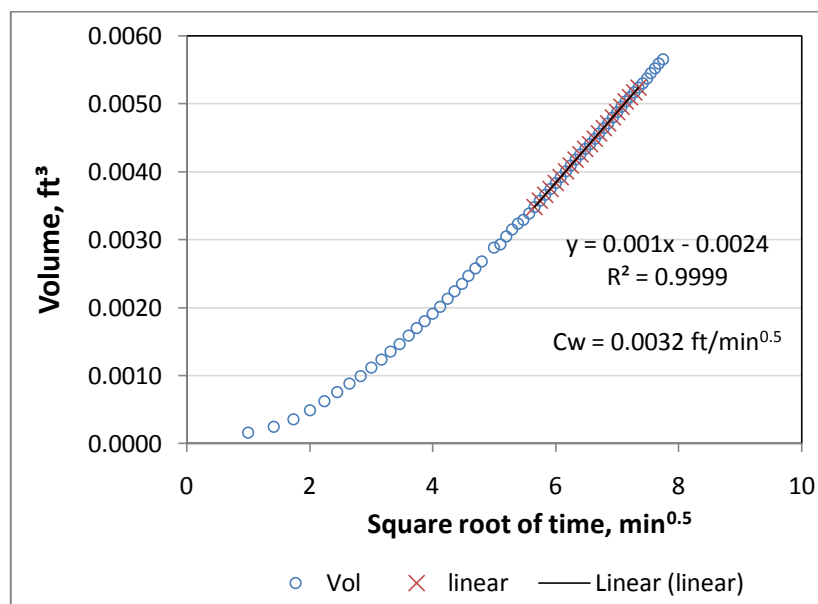


**Fig. 22—Leak off information for experiment E9 with  $C_w = 0.0032 \text{ ft/min}^{0.5}$**

Note that the non-linear early time trend deviates from the normal or expected trend for spurt loss characterized by a high initial leak off rate which drops as the filter cake begins to grow (Fig. 23). This could be because of delayed spurt loss from thick cores with a low permeability (McGowen and Vitthal 1996). All the experiments were run long enough (at least one hour) to observe the linear trend which occurs after spurt

loss from which the leak off coefficient is obtained. Spurt loss usually occurs within the first five minutes.

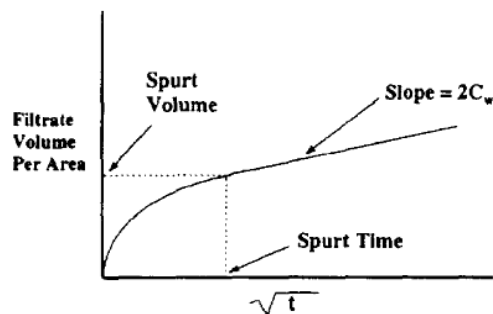


Fig. 23—Classical laboratory leak off data (McGowen 1996)

The effect of shear on fluid loss was also studied and it was observed that as shear rate increased, the fluid loss per unit time as well as the leak off coefficient increased. This is illustrated in Fig. 24 for a set of 60 minute pump time experiments at different shear rates.

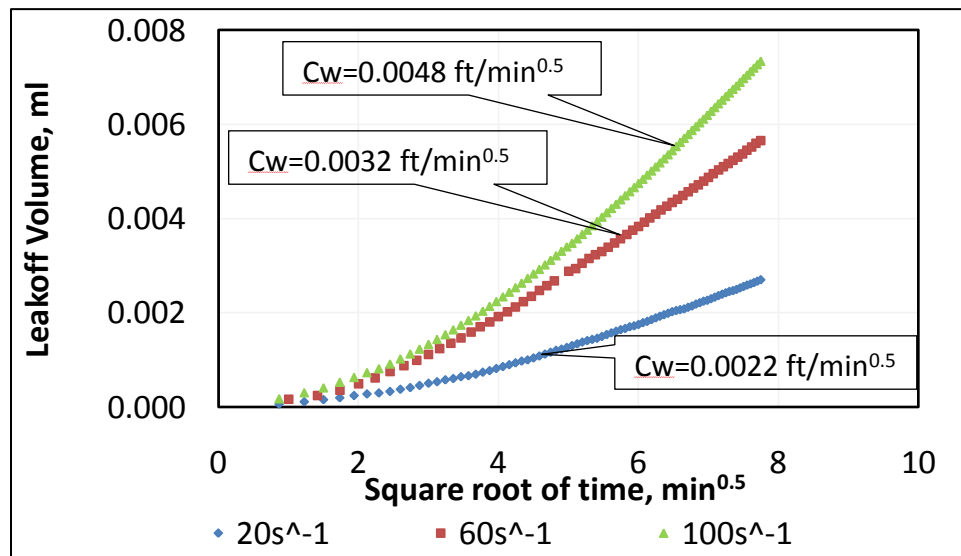


Fig. 24—Effects of shear rate on leak off

In order to estimate the filter cake thickness based on pumping conditions, the leak off coefficient of the rock is required. The leak off coefficient depends on shear rate, net pressure and rock permeability.

To capture the effects of shear rate, the leak off coefficient for each set of experiments was averaged as shown in Table 6.

**Table 6 — Effect of shear rate on leak off coefficient**

Shear Rate $s^{-1}$	Avg. Leakoff Coef $ft/min^{0.5}$	# of data points	Standard Deviation
20	0.002829	5	0.000528
60	0.004018	6	0.000431
100	0.004982	4	0.000584

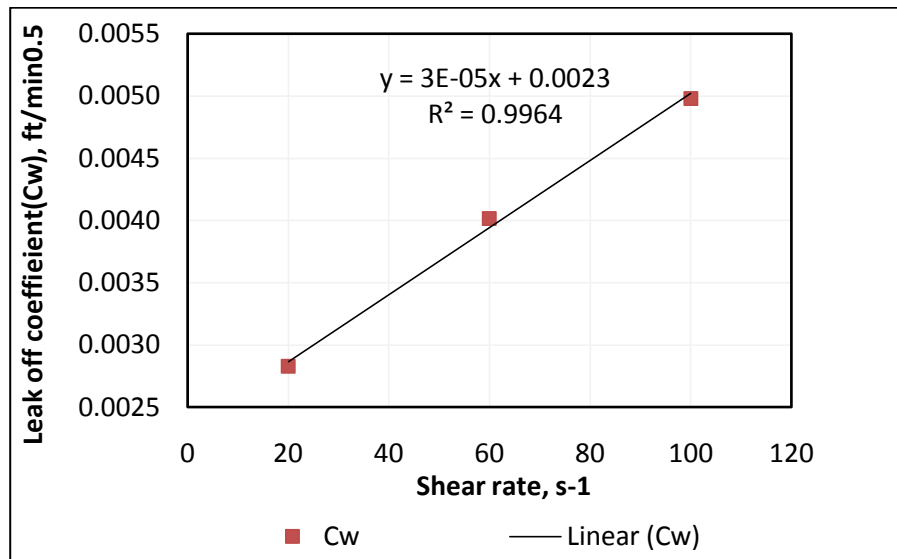


**Fig. 25—Effect of shear rate on leak off coefficient**



#### ***4.2.1 Extension of Results to Conditions Not Tested***

Note that these experiments were run to capture typical field pumping conditions for a 40lb/Mgal gel. To account for larger net pressures and assuming an incompressible filter cake, classical filtration theory stipulates the following relationship between leak off coefficient and pressure (Vitthal and McGowen 1996)

$$C_w \propto \Delta P^{0.5} \quad (4.1)$$

As compressibility of the filter cake increases, the exponent of  $\Delta P$  tends to zero—this makes the leak off coefficient independent of net pressure. This is the typical behavior of borate crosslinked fluids (Vitthal and McGowen 1996).

They also observed that for a crosslinked gel, other than spurt loss, there is no effect of permeability on the leak off coefficient.

#### **4.3 Filter Cake Thickness**

The filter cake thickness for each experiment is obtained as described in subsection 4.1. The laser measurements were verified or compared with a vernier caliper. A close agreement was observed (Fig. 26).

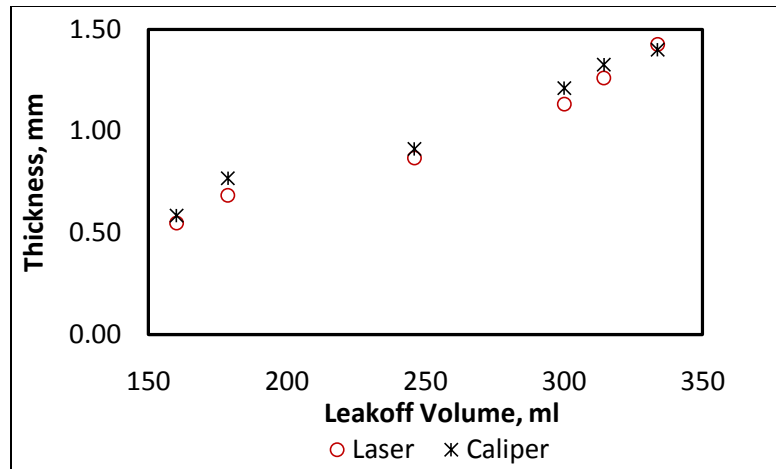


**Fig. 26—Laser and caliper thickness comparison at 60s<sup>-1</sup> shear rate**

The caliper thickness is almost always greater than the laser thickness. This is due to the fact that the caliper measurements referenced the edge of the filter cake which in some cases was apparently thicker whereas the laser averages entire surface. Also, the use of the caliper is subjective hence laser measurements are recommended.

The filter cake thickness for each shear rate category is plotted (Fig. 27).

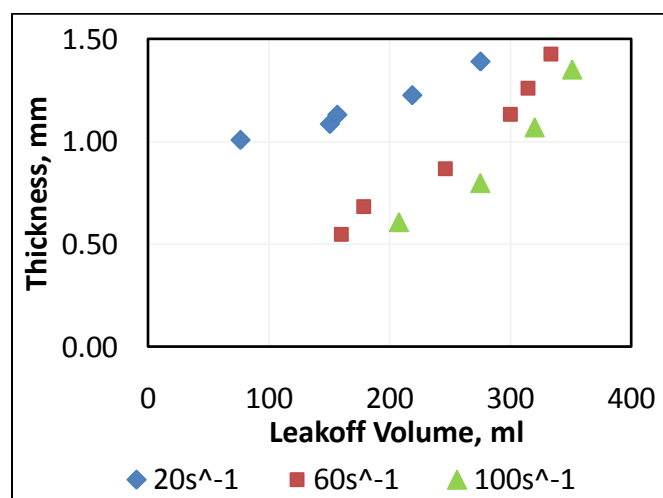


**Fig. 27—Thickness profiles at different shear rates**

The filter cake thickness increases with leak off volume because more polymer solids are deposited and concentrated on the core face as the base fluid (water) leaks off through the rock under pressure. The experiment sets were conducted at three shear rate levels. Each shear rate level yields a constant shear stress. However, the yield stress of the filter cake—which was found to be greater than the shear stress—increases with leak off volume (sub section 4.4). This stress contrast results in an increase in the filter cake thickness as leak off volume increases at each shear level. Viewing the same data across the different shear rates, the filter cake thickness per unit leak off volume is lower at higher shear rates due to erosion of the filter cake from shear.

Static build up tests are conducted by placing a guar crosslinked gel in a conductivity cell, placing caps on the inlet and outlet then applying a closure stress (Xu et al. 2011). The leak off volume is collected and the resulting filter cake thickness is measured using the profilometer. It is also observed in the static test that the filter cake thickness increases as leak off volume increases. However, for the same leak off volume, the resulting static filter cake thickness was greater than the thickness from the dynamic experiments in this work where the gel was subjected to shear. This further confirms that shear rate reduces the buildup of a filter cake residue. Fig. 28 illustrates this effect.

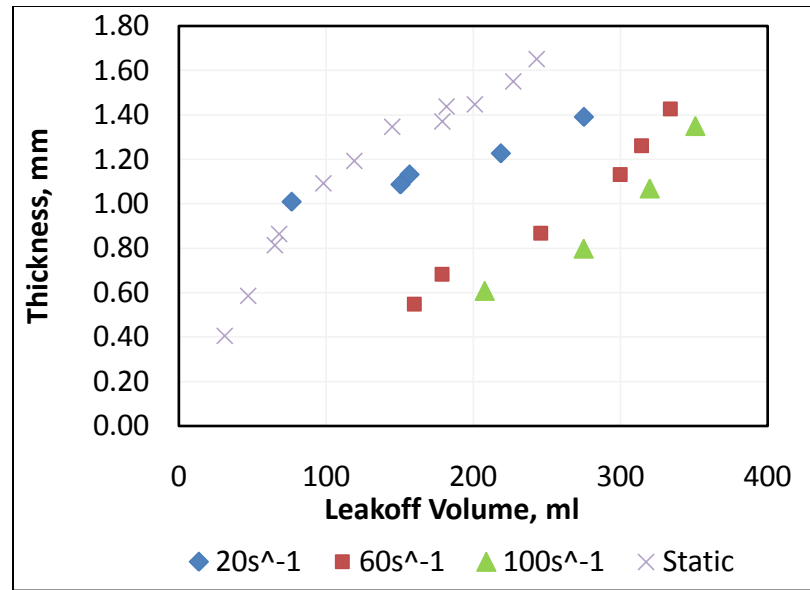


**Fig. 28—Comparison of shear induced vs. static filter cake thickness**

The lower thickness at higher shear rate is mainly accounted for by erosion.

Some of the solids deposited are washed up by the shearing fracture fluid. To corroborate this claim, the experimental data is compared against a model that describes the equilibrium between filter cake formation and erosion (Economides et al. 2003) as shown in Eq. 4.2

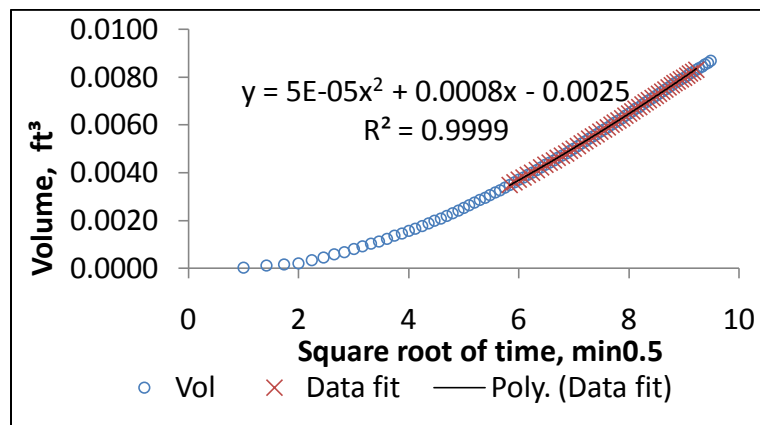
$$u_f = \frac{c}{\sqrt{t}} + 60b\dot{\gamma} \quad (4.2)$$

where  $u_f$  is the filtrate flux,  $C$  is the dynamic fluid loss coefficient for the filter cake,  $t$  is the exposure time (min),  $b$  is a constant accounting for the mechanical stability of the filter cake, and  $\dot{\gamma}$  is the shear rate at the wall ( $s^{-1}$ ). To obtain the corresponding leak off volume, the flow rate (the product of flux and leak off area) is integrated over time to yield leak off volume as shown in Eq. 4.3

$$V_L = 2AC\sqrt{t} + 60Ab\dot{\gamma}t \quad (4.3)$$

Eq 4.3 is a quadratic in terms of  $\sqrt{t}$ . Note that in late time when dynamic equilibrium has been attained, the leak off volume with square root of time also exhibits a strong linear trend (see Fig. 22).

A quadratic regression is plotted using leak off data from the experiments conducted and the resulting coefficients are used to calculate the  $b$  constant. The quadratic fit must be on data AFTER spurt since Eq. 4.3 describes an equilibrium between filter cake build up (happens after spurt) and erosion. It is expected that a good quadratic relationship will be obtained from the leak off data and the value of  $b$  should theoretically be a constant. Fig. 29 shows a quadratic fit from one of the experiments.



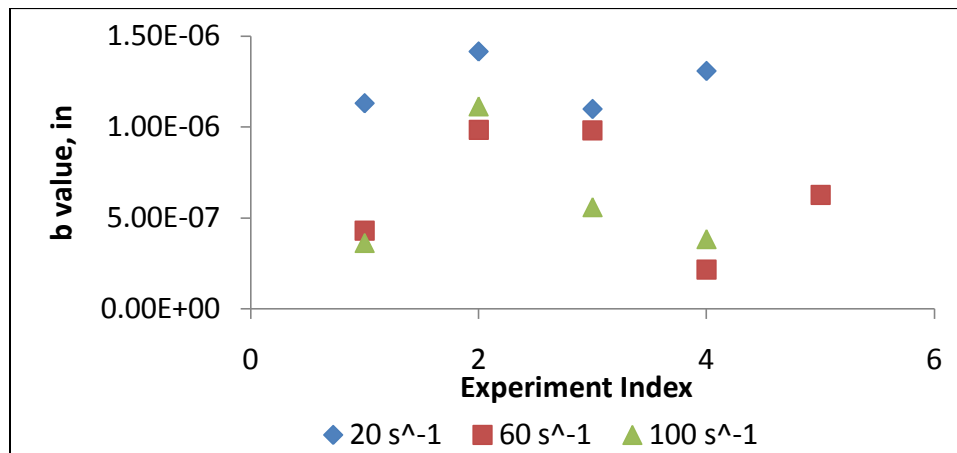
**Fig. 29—Quadratic fit on leak off data**

Fig 29. reveals a strong quadratic fit of the data. This was also observed for other experimental data. The quadratic coefficients are used to calculate the  $b$  value and are tabulated in Table 7.

**Table 7—Experimental determination of filtercake mechanical stability constant**

Shear Rate ( $s^{-1}$ )	Experiment	b value (in)
$20s^{-1}$	E13	1.13E-06
	E7	1.42E-06
	E16	1.10E-06
	E12	1.31E-06
$60s^{-1}$	E9	4.30E-07
	E9B	9.83E-07
	E11	9.81E-07
	E14	2.16E-07
	E14B	6.26E-07
$100s^{-1}$	E15	3.62E-07
	E19	1.11E-06
	E18	5.59E-07
	E17	3.83E-07

The results are plotted as shown on Fig. 30.

**Fig. 30—Experimental determination of filtercake mechanical stability constant**

A significant amount of scatter was observed in the data with a minimum b value of  $2.16E-07$  in. and a maximum of  $1.42E-06$  in. Hassen reported b values for a drilling mud filter cake in the range  $7.87E-09$  to  $1.97E-07$  in. (Hassen 1980). He attributes the

variation to circulation rates or turbulence. In general, higher  $b$  values represent filter cakes that are easily eroded and lower  $b$  values for filter cakes that are harder to erode.

#### 4.3.1 Filter Cake Thickness Model

With the pumping time and anticipated fracture geometry, the leak off volume can be calculated from

$$V_L = 2AC_w\sqrt{t} \quad (4.4)$$

The leak off coefficient,  $C_w$ , is discussed in Section 4.2.

The filter cake thickness is found to have a quadratic relationship with leak off volume (Fig. 31). The eroding effects of shear rate on the thickness as discussed before must be considered (Fig. 28).

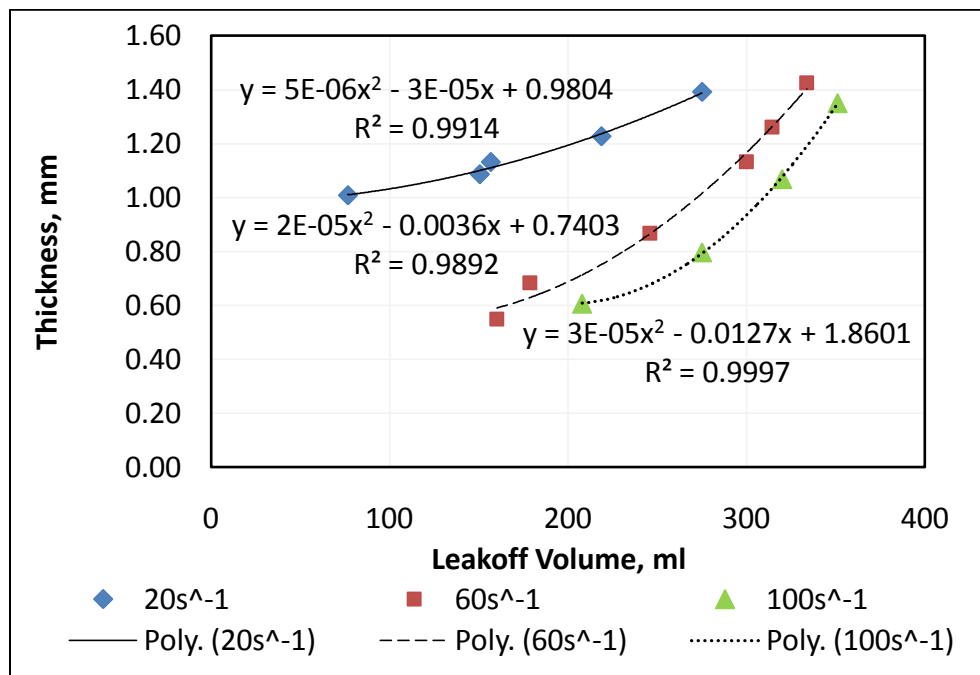


**Fig. 31—Correlations for filter cake thickness**

The experiments account for typical shear rates observed in the field for a 40Lb/Mgal crosslinked gel. If the user encounters different conditions, this data can be extrapolated with discretion. There is a minimum amount of leak off volume (spurt loss) required to begin to generate a filter cake.

Note that in reality, fractures do not have a constant width. The fracture width is largest near the wellbore and smallest at the fracture tip. This results in different shear rates for the same pumping rate within the fracture. This study was performed at different constant shear rates which can be extended to represent the shear rate history along the fracture; i.e., the high shear rate experiments represent what happens near the fracture tip and the low shear rate experiments represent what happens near the wellbore.

#### **4.4 Filter Cake Concentration and Yield Stress**

The concentration of the filter cake is computed using a mass balance. With the concentration of the filter cake known, the corresponding yield stress can be obtained. This is discussed in sub section 2.1.3.

Since it is observed that shear erodes the filter cake, the mass balance has to account for eroded filter cake. This in essence should revert the filter cake thickness to levels with no shear. Data from the static leak off experiments is referenced to calculate the yield stress of the filter cake (Xu et al. 2011). The concentration of the filter cake is plotted against leak off volume as shown in Fig. 32.



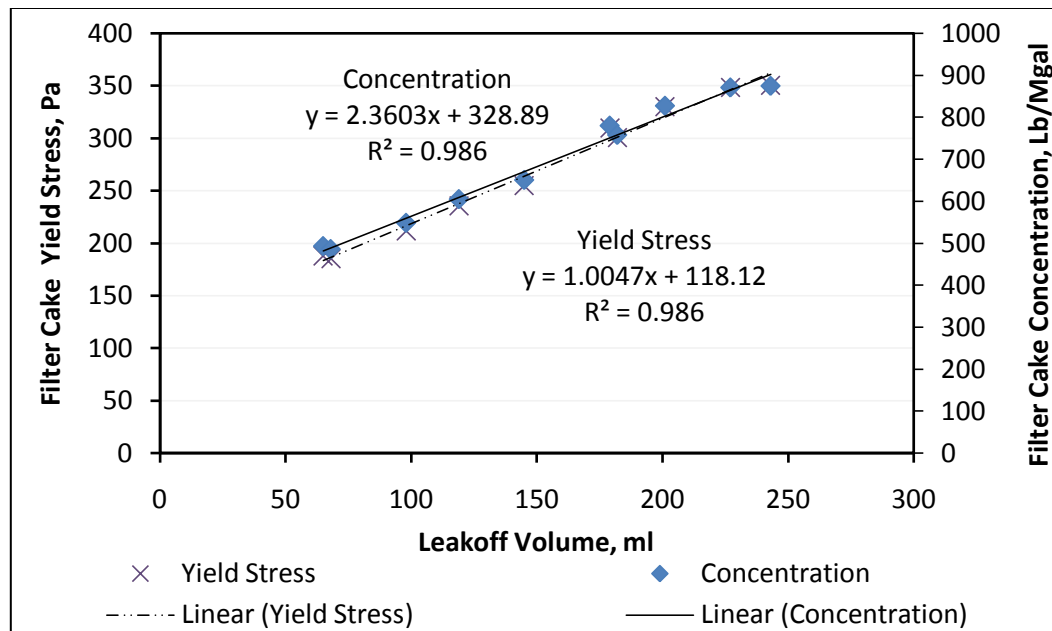


**Fig. 32—Change in concentration and yield stress with leak off**

The concentration of the filter cake increases with leak off volume as expected—more polymer solids are concentrated in the filter cake as leak off increases.

This data can be used to estimate the filter cake concentration for analog pumping conditions

Since the yield stress of the filter cake directly depends on filter cake concentration (Eq. 2.8) a similar trend is observed for the yield stress

#### 4.5 Filter Cake Characterization Workflow

Using the data and trends described in the previous sections, the filter cake can be characterized using the workflow proposed in Fig. 33.

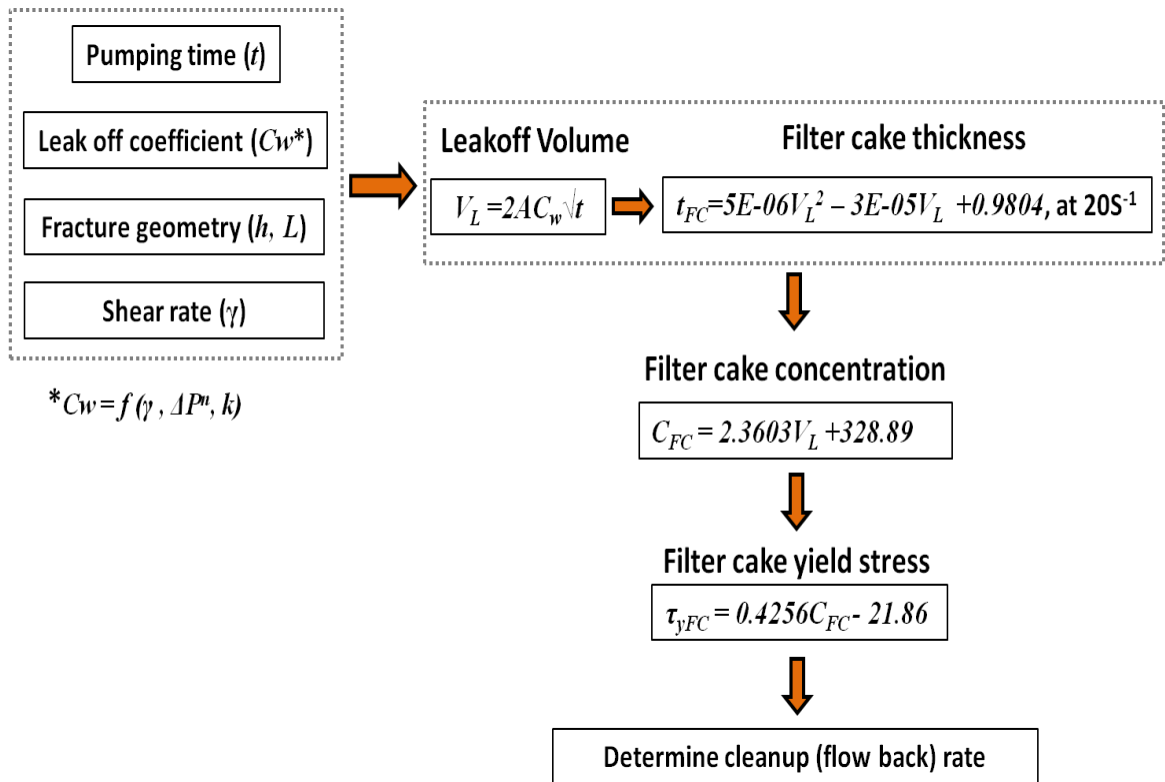


**Fig. 33—Filter cake characterization workflow**

## 4.6 Fracture Performance and Filter Cake Cleanup

The goal of this research work is to characterize the effects of gel damage which provides vital information for fracture clean up.

### 4.6.1 Filter Cake Effects on Fracture Performance

As the filter cake grows (with an increase in leak off volume), the effective fracture width reduces. This in turn reduces the fracture conductivity. For these experiments a loss of fracture width was observed from as low as 9% to as high as 22%. Since it was observed that an increase in shear rate reduces filter cake growth, as

expected, the loss in fracture width decreases with an increase shear rate for the same leak off volume or pumping time (Fig. 34).

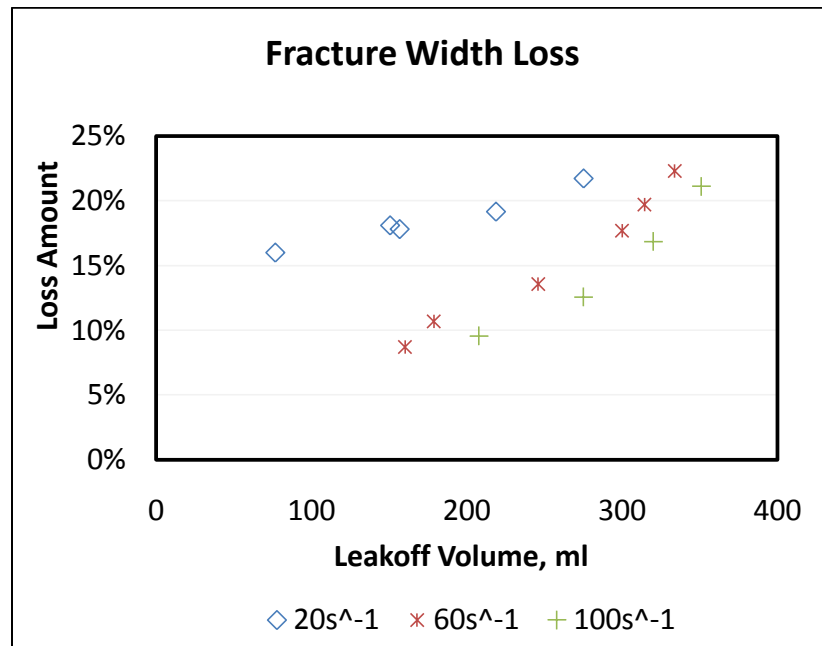


**Fig. 34—Fracture width loss**

#### 4.6.2 Filter Cake Cleanup

The filter cake deposited on the fracture face behaves as a Herschel Bulkley fluid – a non-Newtonian power law fluid having an initial yield stress. To clean up the filter cake, a fluid needs to be pumped at a shear rate which results in a shear stress that exceeds the yield stress of the filter cake. Details of the clean up theory is discussed by Ouyang (Ouyang et al. 2011).

To test the clean up theory, the filter cake was build as described in this work. For simplicity, a 20 s<sup>-1</sup> shear rate experiment was conducted with 90 minutes of build up

time. The buildup properties are tabulated in Table 8. The [expected] values in bold/italic were obtained from the models discussed in the previous sections. For example, using the yield stress equation (Eq 2.8) and data for Experiment E21, we have

$$\begin{aligned}\tau_{y_{FC}} &= 0.4256C_{FC} - 21.8758 \\ &= 0.4256 (748) - 21.8758 = 296.47\text{Pa} \quad (4.5)\end{aligned}$$

**Table 8—Cleanup test data**

Exp't	w (in)	q (ml/s)	Shear Rate (s <sup>-1</sup> )	Leakoff Time (min)	Leakoff Volume (ml)	Thickn ess (mm)	FC Conc (lb/Mgal)	Yield Stress (Pa)	Leakoff Coef ft/min <sup>0.5</sup>
E21	0.250	6.08	20.71	94	177.49	<b>1.1326</b>	<b>748</b>	<b>296</b>	0.0032
E20	0.252	7.3	24.56	90	217.90	<b>1.2113</b>	<b>843</b>	<b>337</b>	0.0037

Water was used as the cleanup fluid. Based on the filter cake properties obtained, a critical water flow rate of 53 ml/s was calculated to erode the filter cake. In order to properly test this model, the water flow rate was increased in steps from 25 ml/s to 62 ml/s as shown in Fig. 35. The duration for each flow rate step was 10 to 15 minutes. Note that there was a separate experiment, E20, run at similar conditions to E21, but eroded at a rate of 70 ml/s. The results are shown in Figs. 35 and 36.

Before cleanup, the fracture space is full of original gel at the center and filter cake on the core faces. When the cleanup flow rate is set to 25 ml/s, the water easily displaces the original gel (at a 40 lb/Mgal concentration with a low yield stress of 0.33 Pa), and creates a channel to the right of the fracture. This is probably due to a relatively “lower resistance” in this area and the clean up flux is too low to displace all the original

gel. As the cleanup rate increases to 40 ml/s, more original gel is displaced creating a wider channel. With the clean up rate increased to 50 ml/s, all the original gel is displaced leaving behind the filter cake which is harder to clean up. The filter cake for this experiment has an estimated concentration of 748 lb/Mgal and yield stress of 296 Pa. When the rate is further increased to 62 ml/s over 85% of the filter cake is eroded (Fig. 35). Finally, at a flow rate of 70 ml/s practically all of the filter cake is eroded. Once the filter cake just begins to move (critical rate), the flow back or clean up can be continued at this rate for a longer period of time for more filter cake to be removed. The critical flow rate for the referenced clean up experiments is estimated at 55 ml/s to 62 ml/s compared to the 53 ml/s theoretical estimate. With the findings from the two experiments conducted, we ascertain that the theoretical model for the filter cake clean up is reasonable given the expected variation between theoretical models and 'field' results.

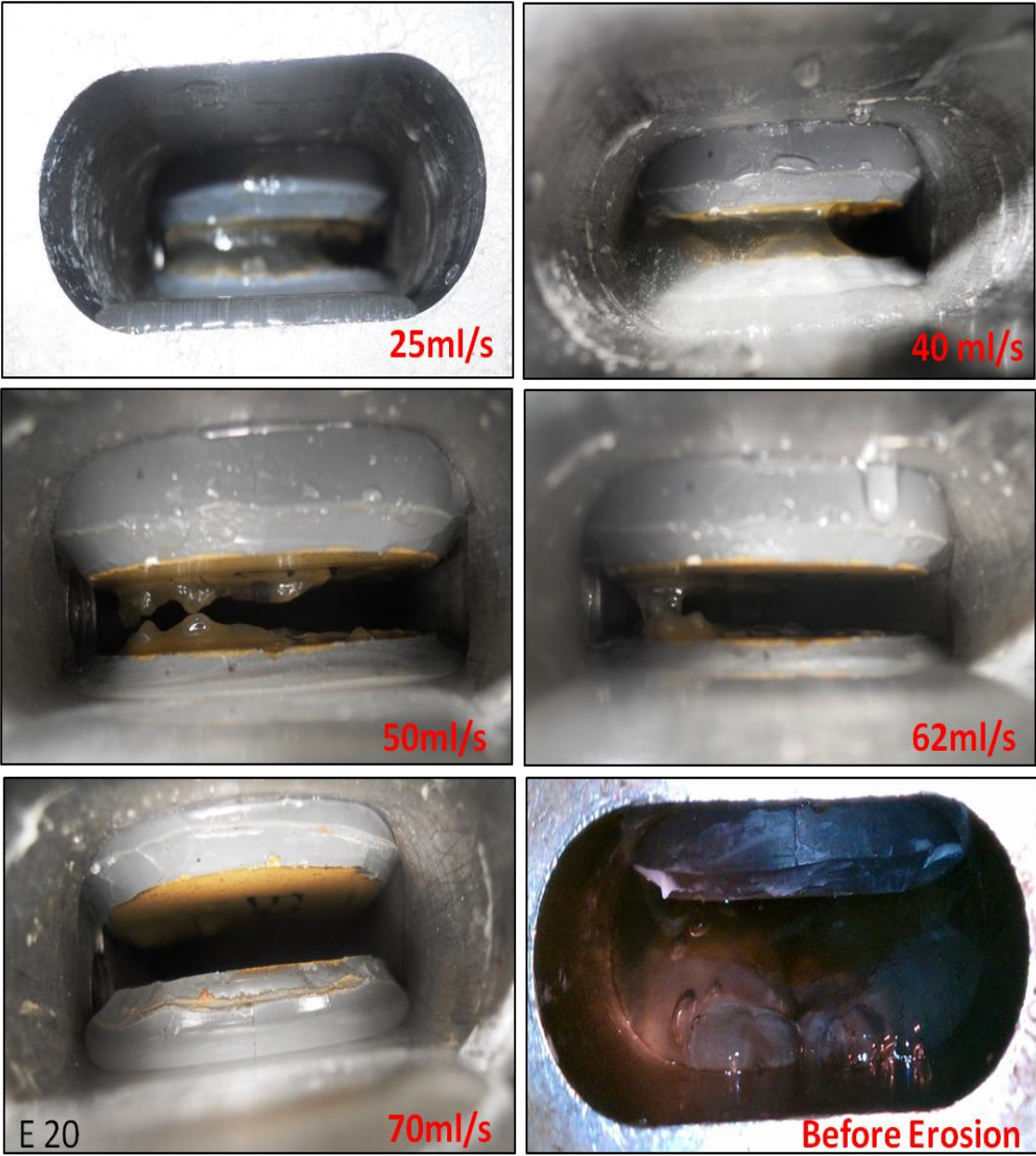
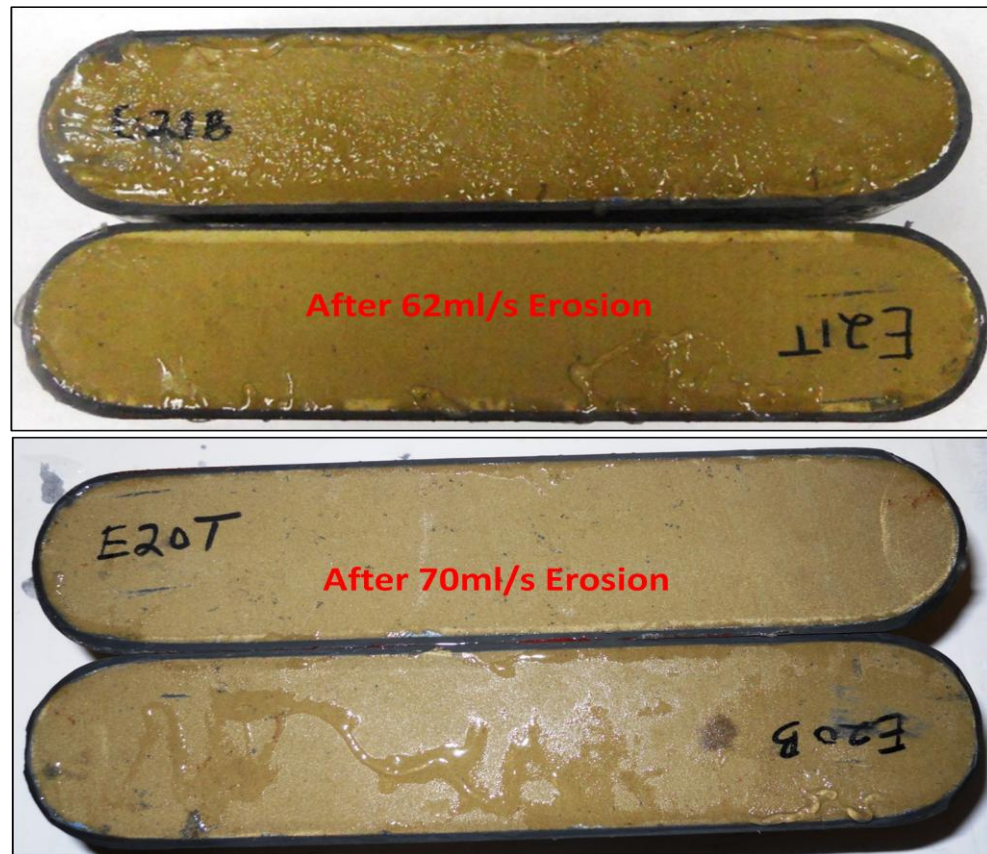


Fig. 35—Step flow erosion test



**Fig. 36—Core surfaces after erosion test**

#### ***4.6.3 Other Cleanup Considerations***

Using a small amount of breaker delivered directly into the filter cake is more effective at reducing the yield stress effects than a larger breaker amount delivered randomly in the slurry. However, when the filter cake occupies a significant fraction of the fracture width with a high concentration, addition of even large concentrations of breaker will not effectively reduce the yield stress (Ayoub et al. 2006). In this case, one would have to rely on flow back to clean the fracture as proposed in this research.

Another increasingly used alternative fracturing fluid is slick water fracturing which uses a very low viscosity fluid to create fractures with no filter cakes. However,

this is limited to naturally fractured low permeability gas reservoirs which have a high unpropped conductivity (King 2010). The slick water systems cannot evenly transport and distribute proppant where propped conductivity is needed.



## 5. CONCLUSIONS AND RECOMMENDATIONS

### 5.1 Conclusions

The main goal of this research was to build up filter cake under dynamic fluid loss conditions and capture the effects shear rate on filter cake properties. These properties include filter cake thickness, concentration and yield stress. The knowledge of the filter cake properties provide useful inputs to design cleanup treatments. The following conclusions are drawn from the study.

1. Filter cake was build up under dynamic conditions with varying shear rates.
2. The filter cake thickness was measured with a laser profilometer. The profilometer readings were checked against a vernier caliper with a close agreement in readings.
3. The filter cake thickness increases as leak off volume increases for each of the various shear rates tested. However, it was found that higher shear rates resulted in relatively lower filter cake thickness. High shear rate impedes the growth of the filter cake as some of the polymer solids deposited are washed off. The relationship between filter cake thickness and leak off volume was found to be quadratic.
4. The filter cake concentration and yield stress increase with an increase in leak off volume as the polymer solids concentrate in the filter cake.
5. A model for the filter cake thickness and properties is developed and can be used in a fracture design model to capture the effects of gel damage. A workflow for the characterization of filter cake build up is proposed.

6. The filter cake properties established for different pumping conditions can be used to design filter cake clean up by flowing back formation fluids at a shear stress that exceeds the yield stress of the filter cake. A theoretical model was tested and validated using water as the flow back fluid. This can be extended to other fluids such as oil or gas with the proper adjustments for fluid properties.
7. High shear rates (typically near the fracture tips) can impede the formation of an external filter cake and also results in higher spurt and fluid loss.
8. The results found can be extended to other pumping conditions as discussed.

## **5.2 Recommendations**

The experiments included several conditions to represent field conditions as close as possible. Instead of pumping just a crosslinked gel, a slurry, which is a combination of proppant and gel should be pumped to better represent field conditions.

Another factor which will be interesting to study is adding the effect of shear degradation of the fracturing fluid in the production tubing before it gets to the formation. This can be achieved by including a tubing loop with diameter and length sized to reproduce shear rates and dwell times in the production tube. The degraded fluid may reduce in viscosity and change leak off behavior.

Including a means of accurately measuring pressure drop in real time within the cell during the pumping of the gel could provide valuable information on the build up process of the filter cake. The filter cake thickness may also be determined in real time

by measuring pressure drop when there is no filter cake and then measuring the increase in pressure drop as the filter cake builds up and reduces fracture width.

The effects of a polymer breaker were not included in this study. The experiments conducted in this work had high polymer concentrations in excess of 450 lb/Mgal from a 40 lb/Mgal initial concentration. It has been shown that a polymer breaker is not effective at high polymer concentrations (Ayoub et al. 2006). However, the effect of a breaker can be studied to set up thresholds where it becomes inefficient.

## NOMENCLATURE

$A$	=	Cross sectional area ( $\text{mm}^2$ )
$c_w$	=	Leak off (wall building) coefficient ( $\text{ft}/\text{min}^{0.5}$ )
$c_i$	=	Initial gel concentration ( $\text{lb}/\text{Mgal}$ )
$c_{FC}$	=	Filter cake concentration ( $\text{lb}/\text{Mgal}$ )
$CF$	=	Concentration factor
$h$	=	Fracture (core) height ( $\text{mm}$ )
$K'$	=	Consistency index ( $\text{lbf}\cdot\text{s}^n/\text{ft}^2$ )
$L$	=	Length of core ( $\text{mm}$ )
$n'$	=	Flow behavior index
$q$	=	Volumetric flow rate ( $\text{mm}^3/\text{s}$ )
$T$	=	Temperature ( $^{\circ}\text{F}$ )
$t_{FC}$	=	Filter cake thickness ( $\text{mm}$ )
$t$	=	Leak off time ( $\text{min}$ )
$\tau_w$	=	Shear stress at filter cake wall ( $\text{Pa}$ )
$\tau_{yFC}$	=	Filter cake yield stress ( $\text{Pa}$ )
$V_L$	=	Leak off volume, $L^3$ ( $\text{mm}^3$ )
$V_{FC}$	=	Filter cake volume ( $\text{mm}^3$ )
$w_f$	=	Fracture width ( $\text{mm}$ )
$\gamma_w$	=	Shear rate at filter cake wall ( $\text{s}^{-1}$ )

## REFERENCES

- Ayoub, J.A., Hutchins, R.D., Bas, F.v.d., Cobianco, S., Emiliani, C.N., et al.: "New Results Improve Fracture Cleanup Characterization and Damage Mitigation", paper SPE 102326 presented at the 2006 SPE Annual Technical Conference and Exhibition in San Antonio, Texas, 24-27 September.
- Economides, M.J., Hill, A.D., and Ehlig-Economides, C. 2003. *Petroleum Production Systems*. Englewood Cliffs, New Jersey: Prentice Hall, PTR. Original edition. ISBN 0-13-658683-X.
- Hassen, B.R.: " New Technique Estimates Drilling Filtrate Invasion", paper SPE 8791 presented at the 1980 SPE Formation Damage Symposium in Bakersfield, California, 28-29 January.
- King, G.E.: "Thirty Years of Gas Shale Fracturing: What Have We Learned?", paper SPE 133456 presented at the 2010 SPE Annual Technical Conference and Exhibition in Florence, Italy, 19-22 September.
- McDaniel, B.W. and Parker, M.A.: " Accurate Design of Fracturing Treatment Requires Conductivity Measurements at Simulated Reservoir Conditions", paper SPE 17541 presented at the SPE Rocky Mountain Regional Meeting, Casper, Wyoming, 11-13 May.
- McGowen, J.M. and Vitthal, S.: "Fracturing-Fluid Leakoff under Dynamic Conditions Part 1: Development of a Realistic Laboratory Testing Procedure", paper SPE 36492 presented at the 1996 SPE Annual Technical Conference and Exhibition, Denver, Colorado, 6-9 October.

- Navarrete, R.C., Cawiezel, K.E., and Constien, V.G.: "Dynamic Fluid Loss in Hydraulic Fracturing under Realistic Shear Conditions in High-Permeability Rocks", *SPE Production & Operations* **11** (3). DOI: 10.2118/28529-pa, 1996
- Ouyang, L., Yango, T., Zhu, D. and Hill, A.D.: "Theoretical and Experimental Modeling of Residual Gel Filter Cake Displacement in Propped Fractures". paper SPE 147692 to be presented at the 2011 SPE Annual Technical Conference and Exhibition, Denver, Colorado, 1-2 November.
- Prud'homme, R.K. and Wang, J.K.: "Filter-Cake Formation of Fracturing Fluids", paper SPE 25207 presented at the 1993 SPE International Symposium on Oilfield Chemistry, New Orleans, Louisiana, 2-5 March.
- Vitthal, S. and McGowen, J.M. "Fracturing Fluid Leakoff under Dynamic Conditions Part 2: Effect of Shear Rate, Permeability, and Pressure", paper SPE 36493 presented at the 1996 SPE Annual Technical Conference and Exhibition, Denver, Colorado, 6-9 October.
- Xu, B., Hill, A.D., Zhu, D. and Hill, A.D.: "Experimental Evaluation of Guar Fracture Fluid Filter Cake Behavior", paper SPE 140686 presented at the 2011 SPE Hydraulic Fracturing Technology Conference, The Woodlands, Texas, 24-26 January.

## APPENDIX

### A.1 – Experiment Data

**Table 9—Experimental data**

	Exp't	w (in)	q (ml/s)	Shear Rate (s <sup>-1</sup> )	Temp. (°F)	Leakoff Time (min)	Leakoff Volume (ml)	Thickness (mm)	Filter Cake Conc. (Lb/Mgal)	Yield Stress Pa	Shear Stress Pa	Leakoff Coef ft/min <sup>0.5</sup>
20s <sup>-1</sup>	E13	0.248	6.54	22.72	73.00	60	76.52	1.0089	510	195	19.04	0.002250
	E7	0.236	6.42	24.53	74.00	90	150.45	1.0867	684	269	21.54	0.002571
	E16	0.250	6.85	23.37	74.00	89	156.60	1.1318	699	275	20.58	0.002571
	E8	0.252	5.82	19.60	73.00	120	218.63	1.2271	845	338	16.61	0.003536
	E12	0.252	5.81	19.65	70.50	150	275.05	1.3912	978	394	14.58	0.003214
60s <sup>-1</sup>	E9	0.248	17.29	59.81	75.00	60	160.09	0.5486	707	279	52.44	0.003214
	E9B	0.252	19.54	65.38	76.00	60	178.66	0.6833	751	298	60.24	0.004179
	E11	0.252	19.55	65.53	75.00	90	245.90	0.8671	909	365	57.17	0.004500
	E14	0.252	17.43	59.53	67.00	120	299.98	1.1320	1037	419	31.86	0.003857
	E14B	0.252	17.93	61.61	65.00	120	314.36	1.2617	1071	434	28.51	0.004500
	E10	0.252	17.90	60.00	75.00	150	333.71	1.4260	1117	453	52.60	0.003857
100s <sup>-1</sup>	E15	0.250	31.00	106.67	70.00	60	207.79	0.6071	819	327	66.32	0.004821
	E19	0.250	30.31	103.82	72.00	90	275.04	0.7976	978	394	73.72	0.005786
	E18	0.250	26.81	92.02	71.00	120	319.95	1.0693	1084	440	61.83	0.004500
	E17	0.252	30.12	100.78	76.00	150	350.99	1.3512	1157	471	90.94	0.004821

## A.2 – Profilometer Data Processing Code

The following code is used to transform the profilometer XYZ column data into an ordered matrix for a 3D surface plot within MS Excel. The code ‘cuts’ out the corner points from the scan so that the rounded edge of the core face remains.

```

Sub generate3Dtable()
Dim i, j, x, y As Integer
Dim L, W, MI, ncol, nrow As Double
L = Sheets("Results Plot").Cells(4, 3)      'Read sample length
W = Sheets("Results Plot").Cells(5, 3)      'Read sample with
MI = Sheets("Results Plot").Cells(6, 3)     'Read measurement interval

'Determine # of columns and rows for data
ncol = L / MI + 1
nrow = W / MI + 1

Sheets("Results Plot").Cells(18, 2) = ncol
Sheets("Results Plot").Cells(19, 2) = nrow

'Initialize table starting point

SPi = 0
SPj = 0
Sheets("Results Plot").Cells(11, 4) = SPi
Sheets("Results Plot").Cells(12, 3) = SPj
For i = 1 To ncol - 1
    SPi = SPi + MI
    Sheets("Results Plot").Cells(11, i + 4) = SPi
Next i
For j = 1 To nrow - 1
    SPj = SPj + MI
    Sheets("Results Plot").Cells(j + 12, 3) = SPj
Next j

'Reading left to right laser scan data

For x = 1 To nrow Step 2
    k = (x - 1) * ncol    'skipping row index start point to appropriate location
    For y = 1 To ncol
        k = k + 1
        z_before = Sheets("Input Data").Cells(k + 9, 3) 'Z after filter cake removed
    
```



```

z_after = Sheets("Input Data").Cells(k + 9, 7)
  'If z_after < 0.6 Or z_after - z_before < 0 Then    'To cut off corner points and
leave rounded edges
  If z_after < 0.6 Then    'To cut off corner points and leave rounded edges
  z = 0
  Else
  z = Sheets("Input Data").Cells(k + 9, 15)
  End If
  Sheets("results plot").Cells(x + 11, y + 3) = z
Next y
Next x

```

'Reading right to left laser scan data

```

For x = 2 To nrow Step 2
  k = x * ncol    'for even rows going R to L
  For y = 1 To ncol
    z_before = Sheets("Input Data").Cells(k + 9, 3) 'Z after filter cake removed
    z_after = Sheets("Input Data").Cells(k + 9, 7)
    'If z_after < 0.6 Or z_after - z_before < 0 Then    'To cut off corner points and
leave rounded edges
    If z_after < 0.6 Then    'To cut off corner points and leave rounded edges
    z = 0
    Else
    z = Sheets("Input Data").Cells(k + 9, 15)
    End If
    Sheets("results plot").Cells(x + 11, y + 3) = z
    k = k - 1
  Next y
Next x

End Sub

```

### A.3 – Profilometer Processed Data Output (Excel Program)

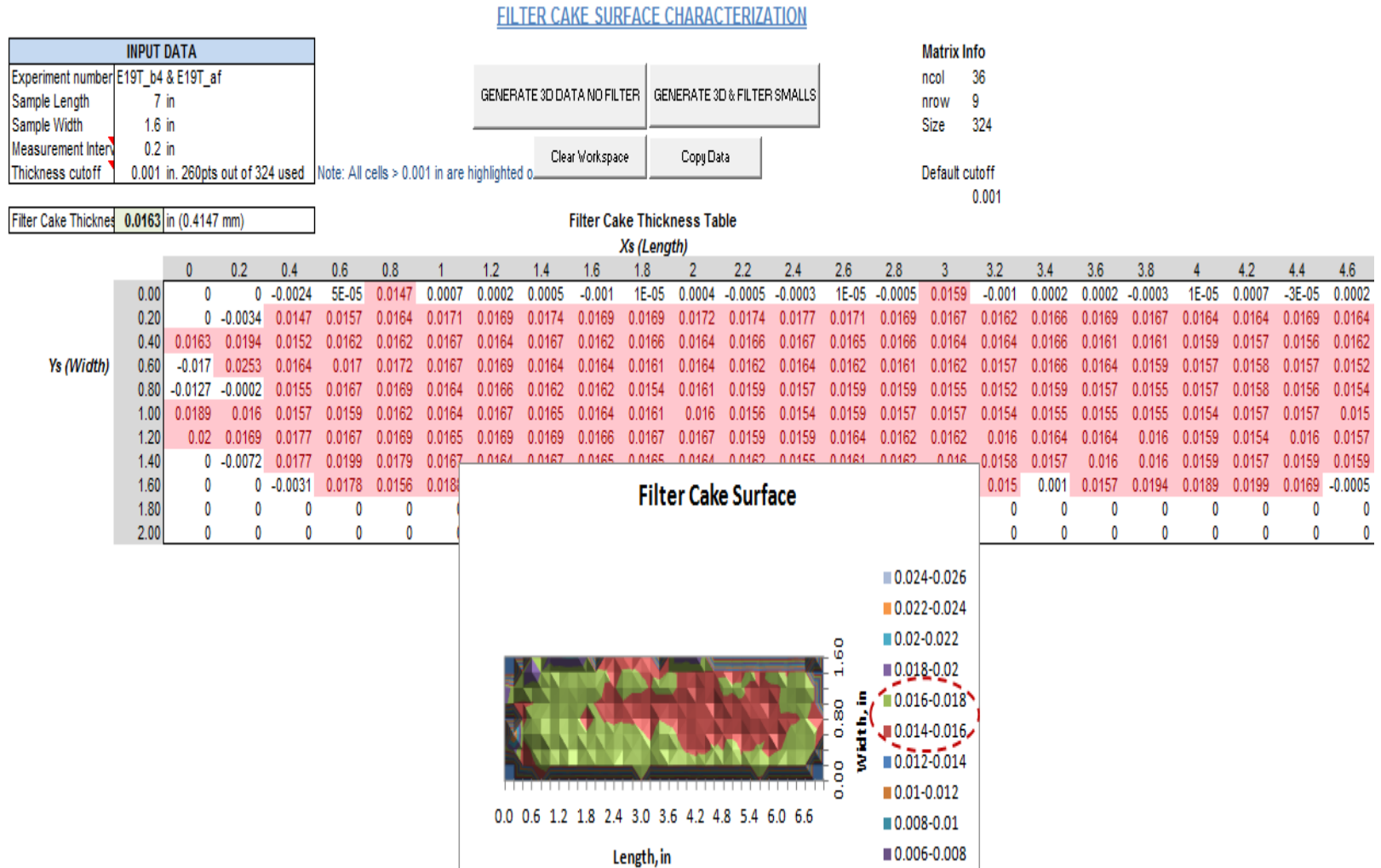


**Fig. 37—Profilometer processed data output in excel**

A.4 – Surface Scans and Pictures

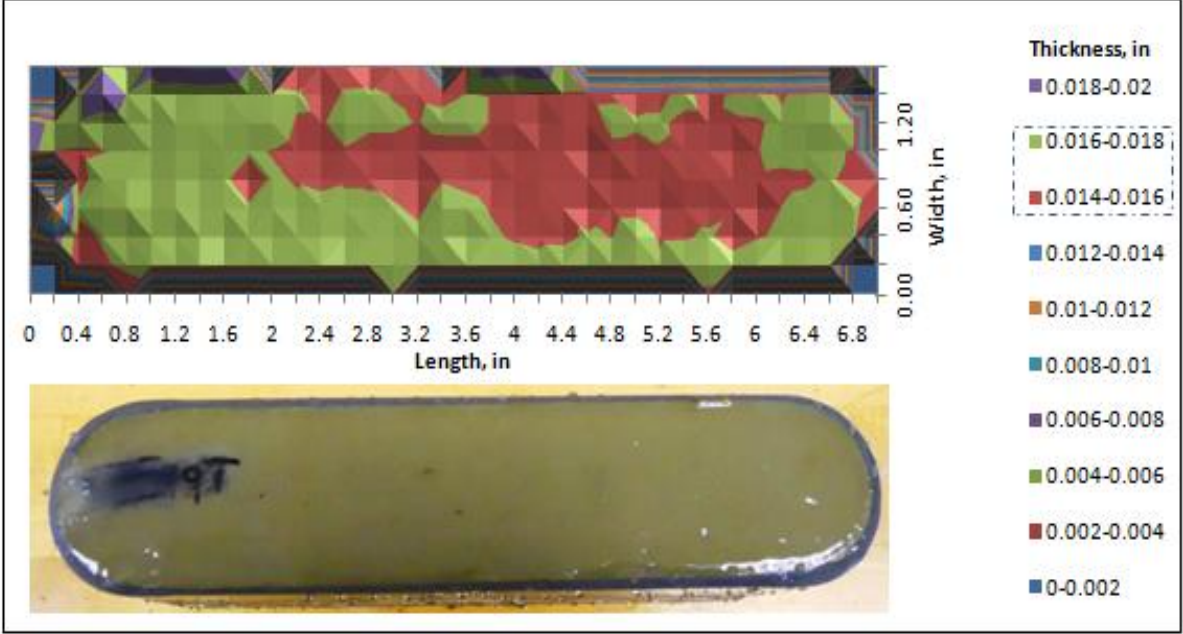


Fig. 38—Experiment E19T top core thickness profile.  $t_{\text{mean}} = 0.0163''$

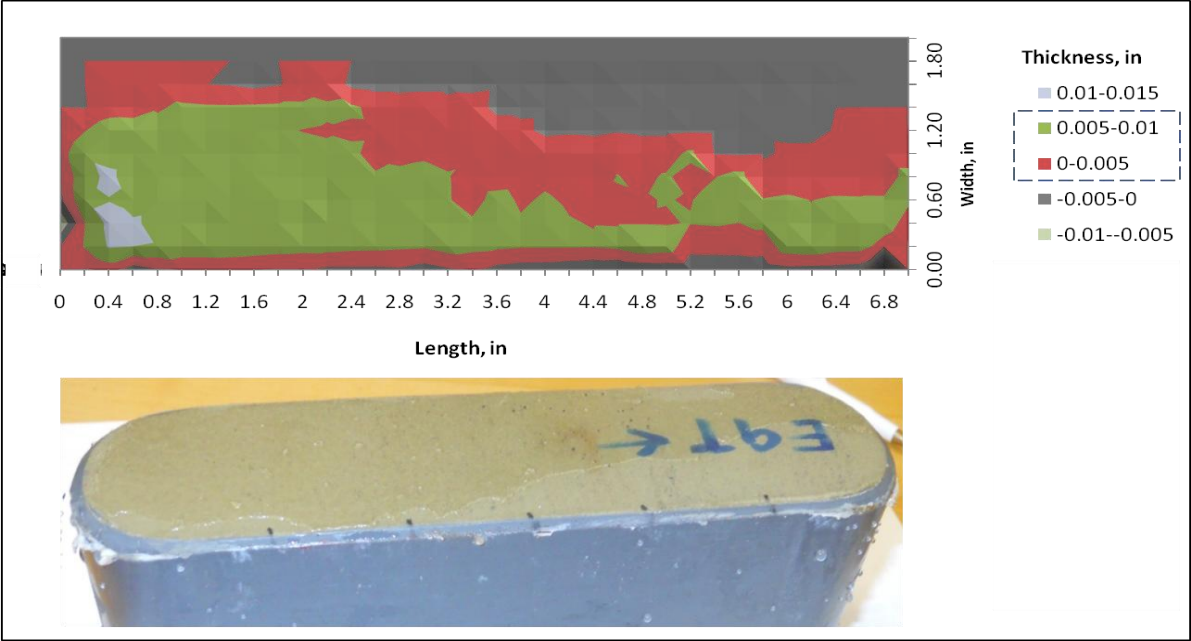


Fig. 39—Experiment E9T top core thickness profile.  $t_{\text{mean}} = 0.008''$

**VITA**

Name: Takwe Yango

Address: Texas A&M University  
Petroleum Engineering Dept.  
3116 TAMU 501 Richardson Bldg  
College Station, TX, 77843

Email Address: takweyango@yahoo.com

Education: B.S., Mechanical Engineering, Oklahoma State University, 2006  
M.S., Petroleum Engineering, Texas A&M University, 2011

This thesis was typed by the author.